Gas-Phase Reactions

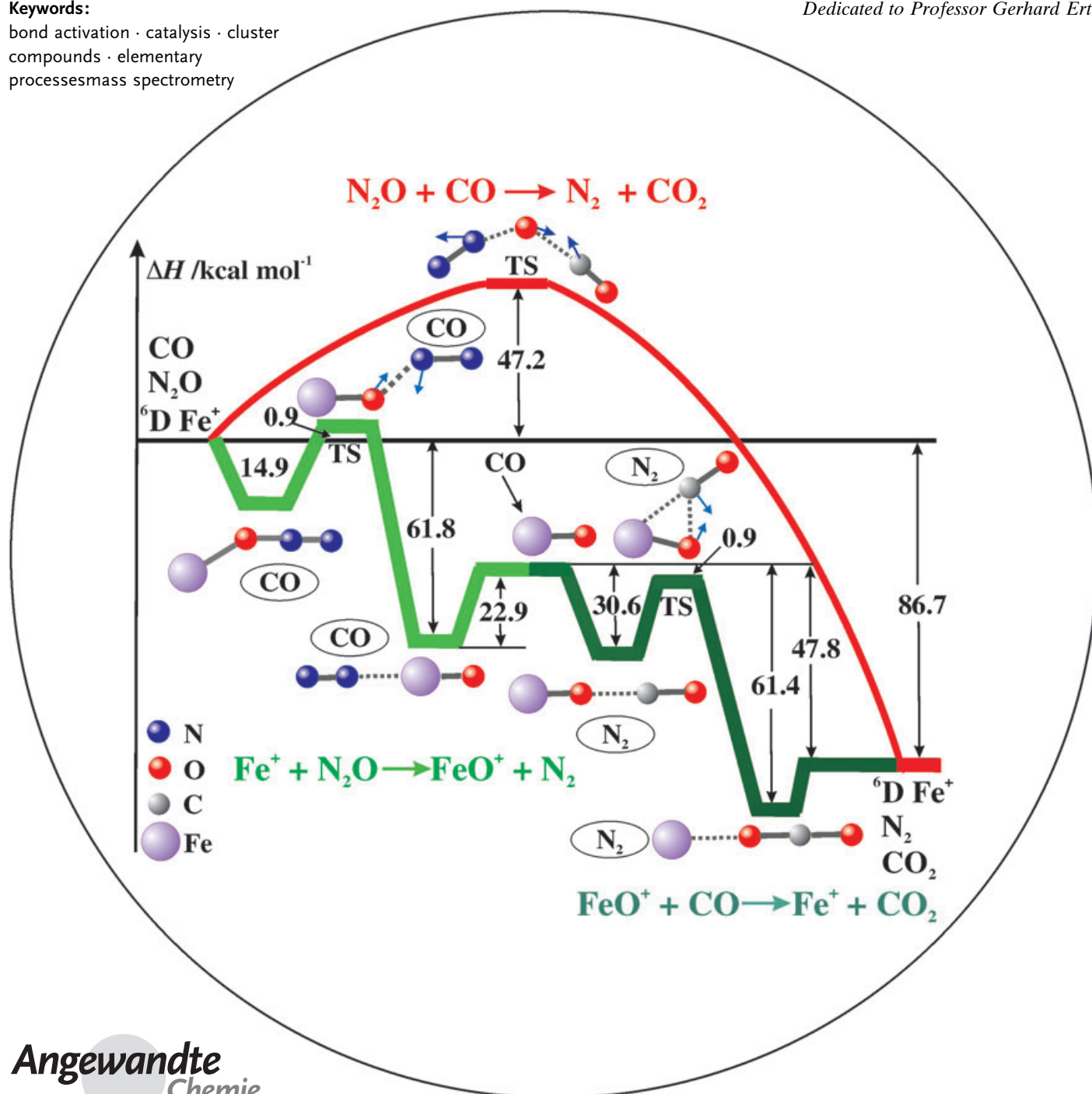# Gas-Phase Catalysis by Atomic and Cluster Metal Ions: The Ultimate Single-Site Catalysts

Diethard K. Böhme* and Helmut Schwarz*

Dedicated to Professor Gerhard Ertl

*G*as-phase experiments with state-of-the-art techniques of mass spectrometry provide detailed insights into numerous elementary processes. The focus of this Review is on elementary reactions of ions that achieve complete catalytic cycles under thermal conditions. The examples chosen cover aspects of catalysis pertinent to areas as diverse as atmospheric chemistry and surface chemistry. We describe how transfer of oxygen atoms, bond activation, and coupling of fragments can be mediated by atomic or cluster metal ions. In some cases truly unexpected analogies of the idealized gas-phase ion catalysis can be drawn with related chemical transformations in solution or the solid state, and so improve our understanding of the intrinsic operation of a practical catalyst at a strictly molecular level.

From the Contents

" *... die Chemie der Gase ist seit einigen Jahren in eine neue Epoche, in das Zeichen der Katalyse getreten. Mit Hilfe von Katalysatoren gelingen die wundersamsten Umwandlungen durch Wasserstoff, Sauerstoff, Stickstoff, Kohlenoxid bei Temperaturen, die viele hundert Grad niedriger sind als diejenigen, bei denen man früher diese Gase reagieren sah. Dieses Kapitel der Katalyse ist schier unbegrenzt ...* **"** [+]

Emil Fischer[1]

1. Introduction

Man-made catalysts contribute substantially to the value of all manufactured goods in industrialized countries;[2] consequently, there are huge efforts to understand and advance the performance of catalysts by uncovering the elementary steps of a catalytic reaction, be it homogeneous (including enzymatic) or heterogeneous. Improving existing catalysts has been identified as one of the three top challenges in contemporary chemistry.[3] However, a tunable catalyst does not exist even for the deceptively simple problem of selective activation and functionalization of an alkane, and resolving mechanistic problems associated with these transformations has proved particularly difficult.[4] This deplorable situation is not really surprising given the enormous complexity of the "real-life situation" in which solvents, counterions, aggregates, or surface inhomogeneities obscure the intrinsic features of a reaction center or the reactive intermediates, the understanding of which is paramount to improving catalysts.

Gas-phase studies on "isolated" reactants provide an ideal arena for detailed experiments of the energetics and kinetics of any bond-making and bond-breaking process at a strictly molecular level. In the last decade mass-spectrometric experiments with advanced techniques have been exploited to provide useful insight into the elementary steps of various catalytic reactions and to characterize reactive intermediates that have previously not been within reach of condensed-phase techniques.[5] Clearly, as a result of the net coulombic charge of the ions studied in a mass spectrometer as well as the absence of counterions and solvation, these coordinatively unsaturated ("naked") species will, in general, be much more reactive than their condensed-phase analogues.[6] Thus, gas-phase studies will, in principle, never account for the precise mechanisms, energetics, and kinetics operating in applied catalysis. However, such experimental studies, complemented by computational investigations, are not at all without meaning, for they provide a conceptual framework and an efficient means to obtain direct insight into reactivity patterns, the role of differential ligation, the importance of aspects of electronic structure, and the nature of crucial intermediates. Furthermore, as these gas-phase studies can be performed under well-defined conditions, they play a key role in the evolution of approaches aimed at a more comprehensive understanding of elementary steps, knowledge of which is mandatory for the design of tailor-made catalysts.[5, 7]

[*] Prof. D. K. Böhme
Department of Chemistry
York University
4700 Keele Street, Toronto, ON, M3J1P3 (Canada)
Fax: (+1) 416-736-5936
E-mail: dkbohme@yorku.ca

Prof. Dr. H. Schwarz
Institut für Chemie
Technische Universität Berlin
Strasse des 17. Juni 135, 10623 Berlin (Germany)
Fax: (+49) 30-314-21102
E-mail: helmut.schwarz@mail.chem.tu-berlin.de

[+] "... the chemistry of gases has entered into a new era in which catalysis has a presence. With help from catalysts, the wonderous transformations involving hydrogen, oxygen, nitrogen, and carbon monoxide can be achieved at temperatures many hundred degrees lower than those at which these gases were observed previously to react. This chapter in catalysis is almost unlimited ..."

In this Review we focus on selected aspects of genuine gas-phase catalytic reactions mediated by atomic metal ions, metal oxide cations, and cluster ions under *thermal conditions*. The emphasis will be on "full thermal catalytic cycles", that is, reaction cycles which start with a bare or a partially ligated, mass-selected metal ion (which can be atomic or a cluster) which adsorbs a neutral reactant molecule, interacts with the other neutral reactant molecule, and then releases product molecules and regenerates the intact precursor metal ion which can start a second cycle—with all events occurring thermally. For the sake of completeness and also to relate to both homogeneous and heterogeneous catalysis, a few systems will be included in which at least one step of the catalytic cycle, for example, the product release, requires supply of external energy which is often provided by collisional activation in the gas-phase experiments.[8] In this Review we will discuss the chemistry of the following three topics: 1) catalysis of oxygen-atom transport, 2) molecular activation with an emphasis on bond-forming reactions, and 3) gas-phase processes which mimic aspects of surface catalysis. We refrain from describing the various experimental techniques, and the interested reader is referred to the original references and leading review articles.[5,6,8]

2. Catalysis of Oxygen-Atom Transport

Many of the catalytic cycles that have been reported to date involve the simple transfer of an oxygen atom from an O-atom donor O−X to an O-atom acceptor Y mediated by an ion $Z^{+/-}$ according to Equations (1) and (2), which result in the overall neutral chemical Reaction (3). Here, X and Y may be inorganic or organic entities. The thermodynamic requirement that must be met by the ionic catalyst $Z^{+/-}$ can be expressed in terms of a "thermodynamic window of opportunity"[9] framed by the oxygen-atom affinities (OA) of the three species involved in Reactions (1) and (2), namely, $OA(X) < OA(Z^{+/-}) < OA(Y)$. This necessary condition results from the fact that only exothermic (or thermoneutral) reactions take place with measurable rate coefficients under thermal conditions in gas-phase processes, provided that no chemical or spin barriers exist beyond the thermochemistry.[10]

$$OX + Z^{+/-} \rightarrow X + OZ^{+/-} \tag{1}$$

$$OZ^{+/-} + Y \rightarrow Z^{+/-} + OY \tag{2}$$

$$OX + Y \rightarrow X + OY \tag{3}$$

The first example of gas-phase catalysis of O-atom transport of which we are aware, although not recognized as such at the time, is the magnesium-mediated destruction of ozone by atomic oxygen, which was reported in 1968 during the study of some fundamental aspects of the chemistry of the earth's ionosphere (E-region):[11] both ion–molecule reactions were measured with the early flowing-afterglow technique and are known to be fast at ambient temperature, with $k_4 = 2.3 \times 10^{-10}$ and $k_5 = 1 \times 10^{-10}$ cm^3 molecule^{-1} s^{-1}.[11] Overall, the atomic Mg$^+$ ion acts as a catalyst in the reduction of ozone by atomic oxygen [Equation (6)], which proceeds with the much smaller rate coefficient $k_6 = 9.1 \times 10^{-15}$ cm^3 molecule^{-1} s^{-1} at room temperature.[12] The origin of this catalytic effect is straightforward: the substantial increase often observed in the rate coefficients of ion–molecule reactions, such as (4) and (5), in contrast to neutral–neutral reactions, such as (6), is a consequence of the electrostatic attraction between ions and molecules that acts to reduce activation energies and thus increase reaction rates.[13]

$$O_3 + Mg^+ \rightarrow O_2 + MgO^+ \tag{4}$$

$$MgO^+ + O \rightarrow Mg^+ + O_2 \tag{5}$$

$$O_3 + O \rightarrow 2\,O_2 \tag{6}$$
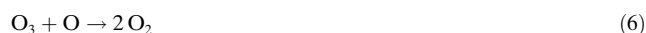
Of interest in terms of atmospheric chemistry at the time was that Reaction (5) keeps the concentrations of Mg$^+$ and MgO$^+$ high in the E-region of the ionosphere where it competes with electron–ion recombination.[11] A variation involving the inefficient direct recombination of oxygen atoms [Equation (10)] has been proposed for the chemistry of Na$^+$ and Fe$^+$ ions at an altitude between 75 and 110 km.[14] The slow, direct attachment of oxygen atoms to the metal ions M$^+$ is circumvented by first coordinating a larger ligand L in a more favorable termolecular fashion [Eq. (7); L = N$_2$, O$_2$, CO$_2$, or H$_2$O]; next, L is exchanged with atomic oxygen in an efficient bimolecular process according to Equation (8). In

Diethard K. Böhme was born in 1941 in Boston and studied chemistry at McGill University (Montreal) where he received his PhD in 1965. In 1969 he moved to York University (Canada), where he has been Distinguished Research Professor since 1994. From 1974–1976 he was an A. P. Sloan Fellow, 1990–1991 a Humboldt Research Awardee, and 1991–1993 a Killam Research Fellow. Since 1975 he has been a Fellow of the Chemical Institute of Canada and since 1994 a member of the Royal Society of Canada. In 2001 he was awarded a Canada Research Chair in Physical Chemistry.

Helmut Schwarz, born in 1943 in Nickenich, has been a professor in Chemistry at the Technische Universität Berlin since 1978. His research interests concern experimental and computational aspects of gas-phase chemistry and physics in their broadest sense and cover chemical systems as diverse as small organic molecules and actinoid polycations. He is the author of more than 800 publications and has given about 700 invited lectures. In 2003 he received the "Otto Hahn Preis für Chemie und Physik". He is a member of several Academies and currently serves as Vice President of the German Research Foundation (DFG).

the final step [Eq. (9)], the metal cation M$^+$ is regenerated reductively, with the overall consequence that the inefficient direct oxygen–oxygen recombination [Eq. (10)] is by-passed by a set of kinetically more favorable ion–molecule reactions. However, this appealing model and its generalization as yet lack experimental confirmation with measurements of the individual rate coefficients.

$$M^+ + L \rightarrow ML^+ \tag{7}$$

$$ML^+ + O \rightarrow MO^+ + L \tag{8}$$

$$MO^+ + O \rightarrow M^+ + O_2 \tag{9}$$

$$O + O \rightarrow O_2 \tag{10}$$
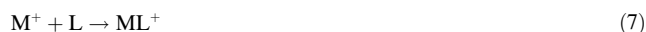
2.1. Reduction of Nitrogen Oxides

Catalytic conversion of harmful gases, such as the oxides of nitrogen produced in fossil-fuel combustion into nitrogen and carbon dioxide, is of utmost importance, both environmentally and economically.[15] CO was one of the first gases investigated for eliminating NO from automobile exhaust gas. While this and other reactions of CO with NO$_n$ ($n = 1, 2$) or N$_2$O are quite exothermic, they do not occur directly to any measurable extent in the gas phase at either room or elevated temperatures. Catalytic converters are required to remove these undesirable pollutants, and metal oxides, mixed metal-oxide compounds, supported metal catalysts, metal zeolites, and alloys have all been investigated as heterogeneous catalysts.

The first example of homogeneous catalysis in the gas phase in which atomic transition-metal cations bring about exothermic reduction of N$_2$O by CO ($\Delta_r H = -87.3$ kcal mol^{-1}) was reported in a landmark experiment by Kappes and Staley in 1981.[16] These authors observed the occurrence, in an ion cyclotron resonance (ICR) mass spectrometer, of Reactions (11) and (12), in which the Fe$^+$ ion transports an oxygen atom from N$_2$O to CO in the overall transformation given by Equation (13). The reported rate coefficients are $k_{11} = 7 \times 10^{-11}$ and $k_{12} = 9 \times 10^{-10}$ cm^3 molecule^{-1} s^{-1}. The oxides of five other transition-metal cations (Ti$^+$, Zr$^+$, V$^+$, Nb$^+$, and Cr$^+$) formed from the bare metal ions and N$_2$O in analogy to Equation (11) were observed not to oxidize CO with a measurable rate, and the findings were ascribed to unfavorable thermochemical features, that is, $D(M^+$-O$) > OA($CO$)$. Refinement of the rate constants of this remarkably simple system were provided in 1995 by selected ion flow tube (SIFT) experiments with $k_{11} = 3.1 \times 10^{-11}$ and $k_{12} = 2.1 \times 10^{-10}$ cm^3 molecule^{-1} s^{-1}, and this study also demonstrated that the cycle defined by Equations (11)–(13) is not poisoned by N$_2$O, since FeO(N$_2$O)$_n^+$ ($n = 0$–3) remains reactive at least up to $n = 3$.[17]

$$N_2O + Fe^+ \rightarrow FeO^+ + N_2 \tag{11}$$

$$FeO^+ + CO \rightarrow Fe^+ + CO_2 \tag{12}$$

$$N_2O + CO \rightarrow N_2 + CO_2 \tag{13}$$

The potential energy curve recently computed for the metal-cation-catalyzed reduction of N$_2$O by CO according to Equations (11)–(13), is shown in Figure 1 for Fe$^+$ (^{6}D).[9] The uncatalyzed process has a computed energy barrier of
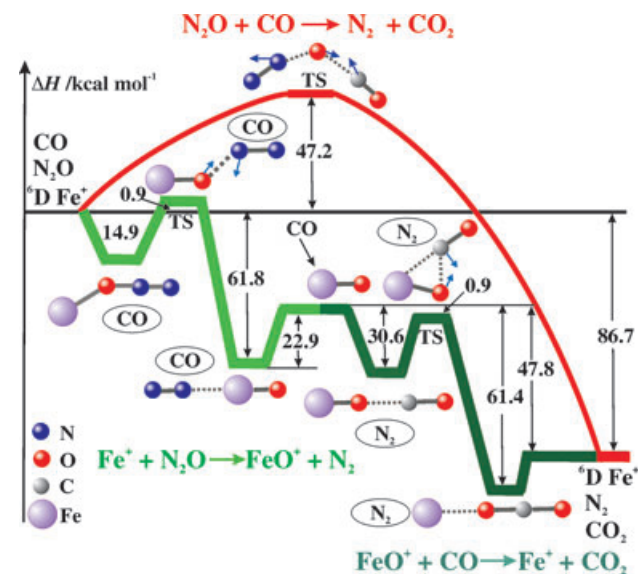

Figure 1. Potential energy curve for the reduction of N$_2$O by CO in the absence and presence of atomic Fe$^+$(^{6}D) computed using DFT with hybrid B3LYP functional and a 6-311+G(d) triple-ζ basis set augmented with one set of diffuse and polarization functions (adapted from ref. [9]).

47.2 kcal mol^{-1}, thus preventing any conversion at elevated temperature despite the process being very exothermic. However, the first step of the much faster ion-catalyzed sequence lowers the energy barrier by more than a factor of 50 to a mere 0.9 kcal mol^{-1}. Both ionic steps in this pathway are described by double-minimum potential-energy profiles that are typical for ion–molecule reactions.[13] The reported differences in the rate coefficients[16,17] arise to a large extent from the energetic features associated with the transition states for the making and breaking of the Fe–O bond.[18]

Atomic Pt$^+$ has also been shown to mediate the reaction of N$_2$O and CO efficiently, with $k = 7 \times 10^{-11}$ for the reduction of N$_2$O and 6.7×10^{-10} cm^3 molecule^{-1} s^{-1} for the oxidation of CO.[19] Recently,[20] the use of inductively coupled plasma/selected-ion flow tube (ICP/SIFT) tandem mass spectrometry[21] has added Os$^+$ and Ir$^+$ ions to the list of catalysts active in the reduction of N$_2$O by CO. This technique has also provided insight into the much more general case,[9] which will be discussed further below. The thermal reactions for the formation of diatomic metal oxides with N$_2$O as an oxidant have been investigated for 59 atomic cations including the fourth-row atomic cations from K$^+$ to Se$^+$, fifth-row cations from Rb$^+$ to Te$^+$ (excluding Tc$^+$), sixth-row atomic ions from Cs$^+$ to Bi$^+$, and the lanthanide cations (excluding Pm$^+$).[22] Primary reactions were observed corresponding to O- and N-atom transfer as well as simple N$_2$O addition. Interestingly, periodicities were noticed in reaction efficiency and these were scrutinized in terms of overall exothermicity, the

presence of a chemical activation barrier in the reaction coordinate, the conservation of spin, and, in the case of lanthanide cations, the energy associated with the promotion of a chemically inert 4f electron to enable formation of a double bond with atomic oxygen (Figure 2). From all the
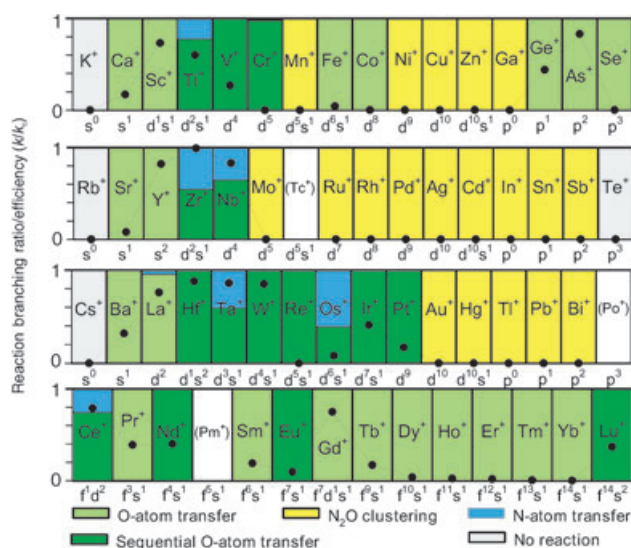
Figure 2. Periodic variations observed in the efficiencies k/k_c (represented as solid circles), for reactions of atomic cations with N_2O. k represents the measured reaction-rate coefficient and k_c is the calculated collision rate coefficient.[23] Also indicated are the observed reaction channels and the ground-state electronic configurations of the atomic cations (adapted from ref. [22a].

cations investigated, 26 atomic systems were shown for the catalysis of O-atom transport to lie within the "thermodynamics window of opportunity" formed by the oxygen affinities of N_2 and CO, with $OA(N_2) = 40$ and $OA(CO) = 127$ kcal mol^{-1}. Catalytic activity was observed with only 10 of these 26 atomic cations, namely Ca$^+$, Fe$^+$, Ge$^+$, Sr$^+$, Ba$^+$, Os$^+$, Ir$^+$, Pt$^+$, Eu$^+$, and Y$^+$. The remaining 16 cations, which meet the thermodynamic criteria for the catalysis of oxygen-atom transport (Cr$^+$, Mn$^+$, Co$^+$, Ni$^+$, Cu$^+$, Se$^+$, Mo$^+$, Ru$^+$, Rh$^+$, Sn$^+$, Te$^+$, Re$^+$, Pb$^+$, Bi$^+$, Tm$^+$, and Lu$^+$), reacted too slowly during either the formation of MO$^+$ or its reduction by CO. As shown earlier,[24] the failure of quite exothermic groundstate O-atom transfer reactions to proceed to a measurable extent at room temperature can often be ascribed in terms of a kinetic barrier resulting from a curve crossing that is required for the change in multiplicity which is necessary for the overall spin to be conserved.[25]

Studies on the role of atomic metal cations in the catalysis of O-atom transport have recently been extended to the oxidation of CO by two other nitrogen oxides, NO and NO$_2$ [see Eqs. (14) and (15)].[20] These processes, together with the reduction of the intermediary diatomic MO$^+$ ions by CO, constitute rare examples of metal-cation-catalyzed reduction of NO$_2$, NO, and N$_2$O coupled with the formation of N$-$N bonds during the termolecular reductive dimerization of NO [Eq. (15)]; overall, NO$_2$ is reduced to N$_2$ [Eq. (16)]. Scheme 1
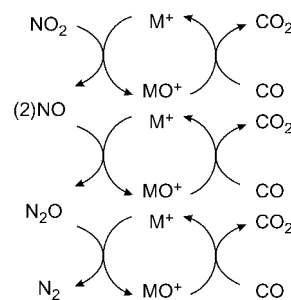
***Scheme 1.*** Reduction with CO and coupling of nitrogen oxides catalyzed by atomic metal cations M$^+$ (M = Fe, Os, Ir; adapted from ref. [20]).

depicts the various cycles involved in this conversion, which has been demonstrated for M$^+$ = Fe$^+$, Os$^+$, and Ir$^+$.[20] Most of the reactions measured correspond to single-channel processes so that the proposed specific catalytic cycles, in principal, have a turnover number of infinity, and thus constitute a "perfect" catalytic cycle. This aspect will be referred to in more detail below.

$$NO_2 + M^+ \rightarrow MO^+ + NO \qquad (14)$$

$$2\,NO + M^+ \rightarrow MO^+ + N_2O \qquad (15)$$

$$2\,NO_2 + 4\,CO \rightarrow N_2 + 4\,CO_2 \qquad (16)$$

Atomic metal cations have also been invoked as catalysts for the reduction of N$_2$O by molecular hydrogen, an exothermic process ($\Delta_r H = -77$ kcal mol^{-1}) which does not occur at ambient temperature in the absence of a catalyst. The thermodynamic window of opportunity in this case is still quite large, $40 < OA(M^+) < 117$ kcal mol^{-1}, and includes 25 atomic cations.[8] The perhaps best studied couple, both experimentally and computationally, concerns the oxidation of H$_2$ by diatomic FeO$^+$ [Eq. (17)].[16,26] This reaction, in conjunction with the formation of FeO$^+$ from bare Fe$^+$ and N$_2$O [Eq. (11)], is remarkable in itself, and among the many salient features the following are worthy of note:

$$H_2 + FeO^+(^6\textstyle\sum{}^+) \rightarrow Fe^+(^6D) + H_2O \qquad (17)$$
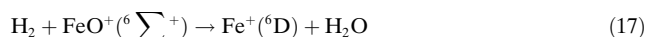
1) Since ground-state atomic Fe$^+$ is inert towards H$_2$ and H$_2$O, and N$_2$O does not react with FeO$^+$ nor with H$_2$ and H$_2$O, the catalytic cycle defined by the combination of Reactions (11) and (17) proceeds with an infinite turnover number; in practice, however, side reactions with background hydrocarbons limit this number to about 100.[5a]
2) The process depicted in Equation (17) is very exothermic ($\Delta_r H = -37$ kcal mol^{-1}), even when excited Fe$^+$(^4F) is formed, which is orbitally unrestricted and spin-allowed. Yet, the reaction efficiency $k/k_c < 1\%$,[26e] which is almost 100 times slower than the reduction of FeO$^+$ with CO [Eq. (12)].
3) The reaction efficiencies for the oxidation of molecular hydrogen by FeO$^+$ show very small intra- and intermolecular kinetic isotope effects for H$_2$, HD, and D$_2$.[16,26a]

4) The most intriguing finding is that the cross-section of Reaction (17) in the vicinity of the threshold slightly diminishes with increasing kinetic energy of the FeO[+] projectile.[26a,e]

Although the small reaction efficiency ($<1\%$) could be interpreted in terms of a classical Arrhenius activation barrier,[17] this assumption perhaps does not seem justified in view of the results of the guided ion beam experiments,[26a,e] which show that the reaction cross-section monotonically decreases with increasing collision energy below 0.2 eV on the center-of-mass scale. Hence, the vanishingly low reactivity of FeO[+] toward molecular hydrogen may well be related to the inefficiency associated with switches between surfaces of different spin, and this scenario is in line with extensive computational studies conducted by Shaik, Schwarz, and co-workers.[26c,d,f,g] The scenario depicted in Figure 3 emerged as
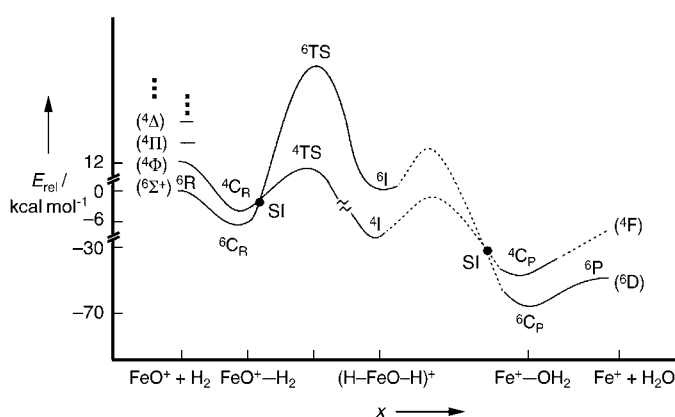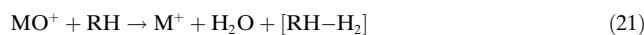

Figure 3. Schematic potential energy profile for Reaction (17). The dashed lines indicate areas not explored computationally. Some energies were taken from refs. [26c, 29]. C_R = reactant complex, SI = spin inversion, I = insertion intermediate, and C_P = product complex (adapted from ref. [26f]).

the most likely description. Two spin-inversion (SI) junctions between the sextet and quartet states occur, one near the FeO[+]/H$_2$ cluster at the entrance channel and one near the Fe^{+}/ H$_2$O complex at the exit. Calculations of the spin-orbit coupling (SOC) indicate a continuous decrease in the SOC value from significant at the entrance to negligibly small at the product exit. The results further show that while the quartet surface provides a low-energy path, the SI junctions reduce the probability of the reaction significantly, and the suggested interplay between spin inversion and chemical barrier height in the FeO[+]-mediated oxidation of molecular hydrogen is confirmed by the pleasing agreement of the experimentally determined (with HD and D$_2$) kinetic isotope effects of Reaction (17) with the computed data.[26e] Clearly, Reaction (17) should not take place at all without the intervention of spin inversion at thermal condition, and the observation of it (although quite inefficient) is both a convincing example for the concept of a "spin-accelerated" transformation[27] as well as a prototype of a two-state reactivity for a thermal process.[25,28,29]

2.2. Oxidation of Hydrocarbons

The principles outlined above for the metal-catalyzed reduction of nitrogen oxides, coupled with the oxidation of CO or H$_2$ by the intermediary MO[+] ions, can also be applied to mediate the oxidation of a hydrocarbon. Equations (18) and (19) show a generalized catalytic cycle for this oxygen-atom transfer, and Equation (20) illustrates how the cycle achieves the oxidation of the hydrocarbon RH. Again, although this oxidation is quite exothermic, no measurable reaction occurs at ambient temperature without the intervention of a catalyst. Mass spectrometric measurements of the kinetics of Reactions (18) and (19) have become straightforward, even when the oxidation of the hydrocarbon [Eq. (19)] produces more than one product and the identification of (ROH) is problematic, if not impossible, by mass-spectrometric means alone. However, in certain cases thermodynamic and mechanistic arguments can be used in the identification of (ROH), particularly in the case of small hydrocarbons. Yet, important alternatives, such as the formation of isomers or the release of water and concomitant dehydrogenation of RH, as shown in Reaction (21), often cannot be excluded.

$$M^+ + N_2O \rightarrow MO^+ + N_2 \qquad (18)$$

$$MO^+ + RH \rightarrow (ROH) + M^+ \qquad (19)$$

$$N_2O + RH \rightarrow (ROH) + N_2 \qquad (20)$$

$$MO^+ + RH \rightarrow M^+ + H_2O + [RH-H_2] \qquad (21)$$

Extensive literature is now available on C–H and C–C bond activation by transition-metal oxide cations in the gas phase.[5a,e,i,29,30] Most of these measurements, at least until recently, have involved Fourier transform ICR mass spectrometry, and the emphasis has been on reactions of MO[+] with M = Fe, as well as a few other metals such as Sc, Ti, V, Cr, Mn, Co, Ni, Os, and Pt. Many of these diatomic metal oxides have been shown to react with a variety of hydrocarbons RH to regenerate M[+], at least in a fraction of the reactive collisions, thus closing the catalytic cycle defined by Equations (18)–(20). This situation has been documented for the following systems:
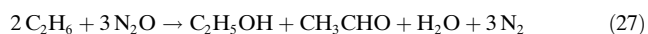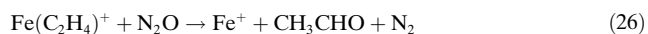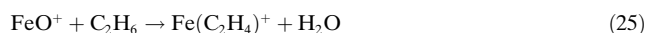
1) FeO[+]/CH$_4$,[26e,31] FeO[+]/C$_2$H$_6$–n-C$_6$H$_{14}$,[32,33] and FeO[+]/ C$_2$H$_2$;[16]

2) reactions of CrO[+],[33] MnO[+],[34] FeO[+],[34,35] CoO[+],[34] NiO[+],[34] and OsO[+][36] with ethane to apparently form acetaldehyde in gas-phase processes which often bridge the gap between heterogeneous metal oxide catalysts and solution-phase oxometal reagents;

3) the fundamentally and industrially important benzene oxidation[37] modeled by reaction of C$_6$H$_6$ with the late transition metal oxide cations CrO[+], MnO[+], FeO[+], CoO[+], and NiO[+] to apparently produce phenol with high efficiencies ($>56\%$).[38] The thermochemical constraints (D(M[+]-O) $> OA$(C$_6$H$_6$)) means that the early transition metal oxide cations ScO[+], TiO[+], and VO[+] do not effect oxidation of benzene; rather, they simply add to the hydrocarbon.[38]

In the following we present in some more detail a few specific examples pertinent to the catalysis of O-atom transfer in the context of hydrocarbon oxidation. Although the conversion of methane into methanol by $FeO^{+[31]}$ [Eq. (22)], has in common with the FeO^+-mediated oxidation of H_2, the feature of two-state reactivity,[25, 28, 39] competitive formation of $FeOH^+$ is substantial [Eq. (23)]. As this ion is unreactive towards methane on thermochemical grounds,[40] the turnover number is limited to the disappointingly small value of 1.6. However, put into a more general perspective, the release of a methyl radical in the course of forming $Fe(OH)^+$ can also be viewed as a model for oxidative coupling of methane.[41] There is a pronounced energy dependence of the branching ratios of Reactions (22) and (23)[26a,b] which deserves a brief mention: Starting from a ratio of 0.4/1 at the lowest kinetic energy, the $Fe^+/Fe(OH)^+$ ratio drops to about 0.03/1 between 0.5 and 1.0 eV, and then increases again, and reaches 1/1 above 5 eV center-of-mass energy.

$$CH_4 + FeO^+ \xrightarrow{57\%} Fe^+ + CH_3OH \qquad (22)$$

$$CH_4 + FeO^+ \xrightarrow{41\%} Fe(OH)^+ + CH_3 \qquad (23)$$
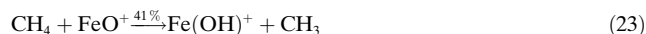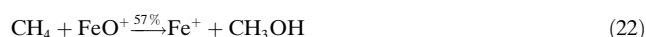
As discussed in detail elsewhere,[25, 26d, 28, 39] formation of CH_3OH is a two-bond process and thus requires the operation of two-state reactivity (TSR). The reactants FeO^+ and CH_4 pass slowly through the crossing region at low kinetic energy, thus allowing the electrons to adjust to a more favorable electronic configuration along the reaction coordinate. Spin inversion from the ground-state sextet entrance channel to a quartet state can take place under such conditions. The latter state provides a low-energy pathway for the formation of Fe^+/CH_3OH in Reaction (22). This reaction declines with increasing kinetic energy since surface crossing becomes less likely at shorter lifetimes of the reactant complexes. The release of a CH_3 radical in Reaction (23) can, however, occur by TSR as well as in a spin-allowed homolytic C—H bond cleavage, which obeys an Arrhenius-type energy dependence and hence dominates at elevated energies. The reaction of FeO^+ with CH_4 has a measured rate coefficient of 2×10^{-10} cm^3 molecule^{-1}s^{-1}, and the kinetic isotope effect analysis favors the insertion species $Fe(CH_3)(OH)^+$ as the intermediate of Reaction (22).[31]

The catalysis of ethane oxidation by Fe^+/N_2O, as illustrated by Reactions (11a) and (24)–(27), is analogous to that of methane except that the channel represented by the formation of C_2H_5OH is now less competitive: rather, the thermochemically favored elimination of H_2O to produce $Fe(C_2H_4)^+$ now comprises 70%,[32] (67%[33]) with Fe^+ formation accounting for only 10%[32] (12%[33]) with $k_{24} = 1 \times 10^{-10}$ cm^3 molecule^{-1}s^{-1}.[33]

$$2 N_2O + 2 Fe^+ \rightarrow 2 FeO^+ + 2 N_2 \qquad (11a)$$

$$FeO^+ + C_2H_6 \rightarrow Fe^+ + C_2H_5OH \qquad (24)$$

$$FeO^+ + C_2H_6 \rightarrow Fe(C_2H_4)^+ + H_2O \qquad (25)$$

$$Fe(C_2H_4)^+ + N_2O \rightarrow Fe^+ + CH_3CHO + N_2 \qquad (26)$$

$$2 C_2H_6 + 3 N_2O \rightarrow C_2H_5OH + CH_3CHO + H_2O + 3 N_2 \qquad (27)$$

$Fe(C_2H_4)^+$, which is formed as a major product in Reaction (25), is not lost for catalysis since it reacts further with N_2O to regenerate Fe^+ in 72% of its reactive collisions [Eq. (26)] and so becomes part of the parallel three-step catalytic cycle shown in Scheme 2.[35] The turnover number of
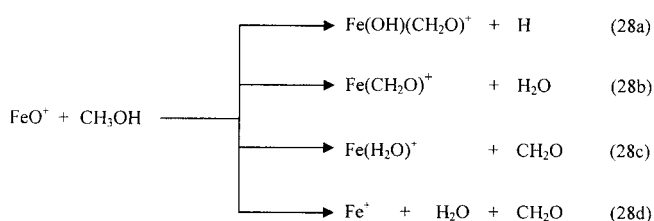

$$C_2H_6 + 2 N_2O \longrightarrow CH_3CHO + H_2O + 2 N_2$$

$$\Delta_r H = -116.5 \text{ kcal mol}^{-1}$$
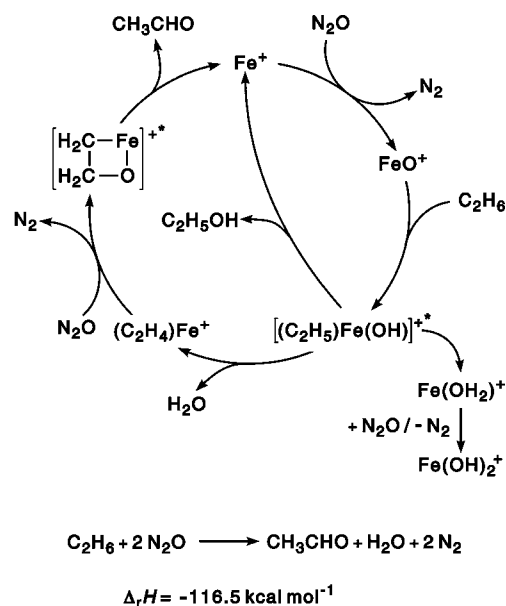
Scheme 2. Catalytic cycle for the Fe^+-mediated oxidation of C_2H_6 by N_2O (adapted from ref. [35]).

the Fe^+-mediated oxidation of C_2H_6 is about 2.5, and the inefficiency in the catalytic cycle is caused by the irreversible formation of $Fe(OH)_2^+$ as a side product. The nonreactivity of this Fe^{III} ion towards ethane emphasizes the essential function of the metal-oxide moiety in FeO^+, rather than the formal iron(III) oxidation state. However, as $Fe(OH)_2^+$ can be converted into $FeO(H_2O)^+$, the reactive species might be regenerated by loss of water upon "heating", that is, collisional activation. This finding actually illustrates, to some extent, an analogy to applied catalytic processes in which desorption of the product (in this case, loss of the water ligand) is often rate-limiting; in practice, dehydration is achieved by performing the oxidation at elevated temperatures. We will return to this aspect of regenerating the active site in a catalytic gas-phase cycle by collisional activation below.
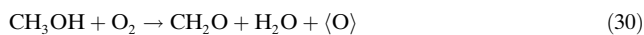
Parallel three-step catalytic cycles may also occur in the catalytic oxidation of alcohols in which production of Fe^+ [Equation (28d)] is a relatively minor channel in the reaction with FeO^+, but which often produces significant amounts of carbonyl-Fe^+ and other Fe^+ complexes.[42] Reaction (28) illustrates the products formed from the oxidation of methanol as an example.

The branching ratio for Reaction (28) is (a)/(b)/(c)/(d) = 0.35/0.35/0.10/0.20, and hence only 20% of the products regenerate the Fe^+ catalyst directly. However, in channels 28b and 28c the Fe^+ complexes $Fe(CH_2O)^+$ and $Fe(H_2O)^+$ are formed and if these both react with N_2O, upon release of the ligands CH_2O and H_2O, the "catalyst" FeO^+ is

$$\text{FeO}^+ + \text{CH}_3\text{OH} \longrightarrow \begin{cases} \text{Fe(OH)(CH}_2\text{O)}^+ + \text{H} & (28a) \\ \text{Fe(CH}_2\text{O)}^+ + \text{H}_2\text{O} & (28b) \\ \text{Fe(H}_2\text{O)}^+ + \text{CH}_2\text{O} & (28c) \\ \text{Fe}^+ + \text{H}_2\text{O} + \text{CH}_2\text{O} & (28d) \end{cases}$$
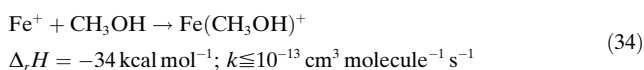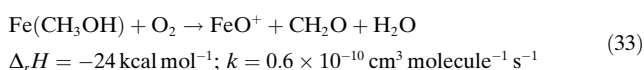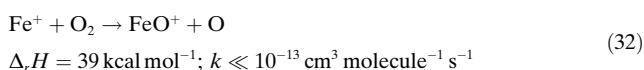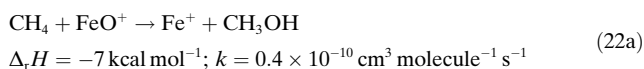
recovered in 45% yield and ready to enter a parallel three-step catalytic chain, in analogy to the $\text{Fe}^+/\text{N}_2\text{O}/\text{C}_2\text{H}_6$ system discussed above.

An attractive variant has been reported for the Fe^+-catalyzed oxidation of methane that involves the conversion of methane into formaldehyde by O_2 in the presence of methanol as a co-catalyst,[43,44] Oxygen-atom transport may proceed both with the formation of formaldehyde from methanol with O_2 as the O-atom donor for Fe^+ and in the oxidation of methane to methanol with FeO^+ [Eqs. (29)–(31)].

$$\text{CH}_4 + \langle\text{O}\rangle \rightarrow \text{CH}_3\text{OH} \tag{29}$$

$$\text{CH}_3\text{OH} + \text{O}_2 \rightarrow \text{CH}_2\text{O} + \text{H}_2\text{O} + \langle\text{O}\rangle \tag{30}$$

$$\text{CH}_4 + \text{O}_2 \rightarrow \text{CH}_2\text{O} + \text{H}_2\text{O} \tag{31}$$

The key gas-phase experiments that mimic the overall Reaction (31) are summarized in Equations (22a) and (32)–(34). The $\langle\text{O}\rangle$ equivalent of Reaction (29) is provided by FeO^+. Since FeO^+ cannot be generated directly from the Fe^+/O_2 couple on thermochemical grounds,[45] the decisive experiment is a methanol-mediated activation of dioxygen in which the alcohol serves as a co-reductant [Eq. (33)]. While this process is quite exothermic ($\Delta_r H = -24\ \text{kcal mol}^{-1}$), the rate efficiency is only about 10%, as a result of spin barriers.[25,42,46]

$$\begin{aligned} &\text{CH}_4 + \text{FeO}^+ \rightarrow \text{Fe}^+ + \text{CH}_3\text{OH} \\ &\Delta_r H = -7\ \text{kcal mol}^{-1};\ k = 0.4 \times 10^{-10}\ \text{cm}^3\ \text{molecule}^{-1}\ \text{s}^{-1} \end{aligned} \tag{22a}$$

$$\begin{aligned} &\text{Fe}^+ + \text{O}_2 \rightarrow \text{FeO}^+ + \text{O} \\ &\Delta_r H = 39\ \text{kcal mol}^{-1};\ k \ll 10^{-13}\ \text{cm}^3\ \text{molecule}^{-1}\ \text{s}^{-1} \end{aligned} \tag{32}$$

$$\begin{aligned} &\text{Fe(CH}_3\text{OH)} + \text{O}_2 \rightarrow \text{FeO}^+ + \text{CH}_2\text{O} + \text{H}_2\text{O} \\ &\Delta_r H = -24\ \text{kcal mol}^{-1};\ k = 0.6 \times 10^{-10}\ \text{cm}^3\ \text{molecule}^{-1}\ \text{s}^{-1} \end{aligned} \tag{33}$$

$$\begin{aligned} &\text{Fe}^+ + \text{CH}_3\text{OH} \rightarrow \text{Fe(CH}_3\text{OH)}^+ \\ &\Delta_r H = -34\ \text{kcal mol}^{-1};\ k \leqq 10^{-13}\ \text{cm}^3\ \text{molecule}^{-1}\ \text{s}^{-1} \end{aligned} \tag{34}$$

Combination of these steps leads to a viable sequence for the Fe^+-mediated oxidation of CH_4 to CH_2O according to Reaction (31). Here, the CH_3OH molecule coordinated to the metal plays a central role both as a precursor for the oxidation product CH_2O as well as a crucial intermediate in the activation of O_2 (Scheme 3). Furthermore, the formation of FeO^+ in Reaction (33) is quite remarkable in that over-oxidation (namely, the formation of Fe^+ and HCOOH) does not occur in this experiment, even though bare FeO^+ rapidly reacts with formaldehyde.[47] The seemingly most simple step in Scheme 3, that is, the mere complexation of methanol by
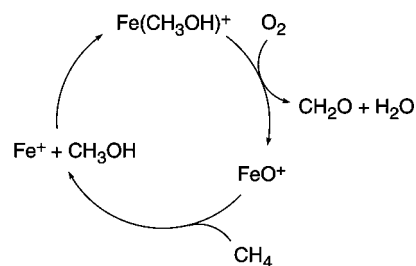

Scheme 3. Catalytic sequence for the Fe^+-mediated oxidation of methane by molecular oxygen with methanol as a catalytic co-reductant. The side reaction of the FeO^+/CH_4 couple, which leads to $\text{FeOH}^+/\text{CH}_3$ [Eq. (23)] is omitted for clarity (adapted from ref. [43]).

the iron cation [Eq. (34)], however, does not occur in the low pressure regime (typically below 10^{-7} mbar). However, the magnitude of k_{34} will be enhanced with increasing pressure since ligand association often proceeds by termolecular collisions.

2.3. Ligand Effects

The influence of ligation of a metal-ion catalyst on the rates and products of oxygen-atom-transfer catalysis is also of interest.[5a] FTICR experiments have noted that ligation of a metal cation with an appropriate ligand can "enhance the selectivity at the expense of reactivity",[48] and the gas-phase chemistry of FeO^+ may serve as a good example: although "naked" FeO^+ behaves as a powerful reagent for the activation of C–C and C–H bonds[5a] and also effects product isomerization, that is, olefin→epoxide→aldehyde conversion, during the course of an oxidation, ligated species Fe(L)O^+ (L = ligand) are entirely unreactive towards bond activation.[48] In contrast, oxygen transfer from Fe(L)O^+ to olefins [Eq. (35)] occurs at the collision rate with less than 10% formation of by-products, and indirect evidence suggests that epoxides rather than ketones or aldehydes are formed. The Fe(L)O^+ catalyst itself can be conveniently regenerated by treating Fe(L)^+ with N_2O [Eq. (36)], with an efficiency ranging from 40–86% depending on L. Thus, Reactions (35) and (36) can be combined in a catalytic cycle (Scheme 4); in the case of L = benzene, turnover numbers of up to 6 are obtained.[48] Related ligand effects were also reported recently for the oxidation of the unsaturated hydrocarbons
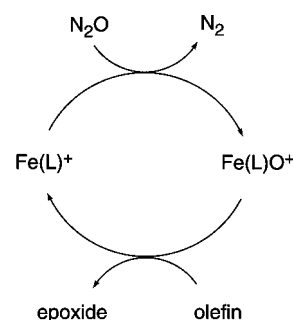
Scheme 4. Catalytic epoxidation of olefins by Fe(L)O^+ complexes (adapted from ref. [48]).

ethene, propene, and benzene by [(phenanthroline)CuO]⁺ which, in contrast to "naked" CuO⁺, brings about almost exclusive transfer of an oxygen atom.[49]

$$Fe(L)O^+ + olefin \rightarrow Fe(L)^+ + epoxide \qquad (35)$$
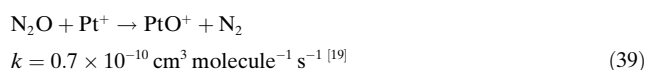
$$Fe(L)^+ + N_2O \rightarrow Fe(L)O^+ + N_2 \qquad (36)$$
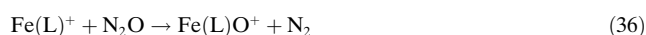
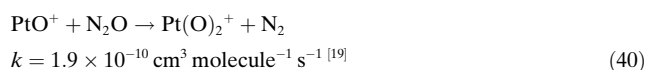### 2.4. Catalysis of O-Atom Transport with Metal Oxide Cations

Dioxide and higher oxide cations with appropriate O-atom affinities may also possess the thermodynamic potential to catalyze O-atom transport. Equations (37) and (38) illustrate the MO_n^+-catalyzed ($n = 1, 2$) reduction of N_2O by CO.
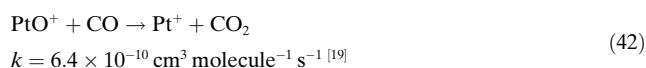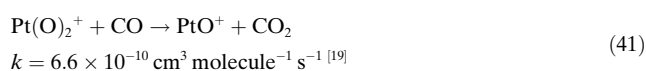
$$N_2O + MO_n^+ \rightarrow MO_{n+1}^+ + N_2 \qquad (37)$$

$$MO_{n+1}^+ + CO \rightarrow MO_n^+ + CO_2 \qquad (38)$$

The "thermodynamic window of opportunity" now becomes $OA(N_2) < OA(MO_n^+) < OA(CO)$ and has been shown to contain a number of metal oxide cations. For example, atomic Pt⁺ is readily oxidized sequentially to form PtO⁺ and $Pt(O)_2^+$ [Eqs. (39) and (40)], and both oxides are efficiently reduced by CO [Eqs. (41) and (42)],[19,22a] with oxygen affinities $OA(Pt^+) = 75$ kcal mol⁻¹ [50] and $OA(PtO^+) = 71$ kcal mol⁻¹ [51] which lie almost in the middle of the thermodynamic window.

$$N_2O + Pt^+ \rightarrow PtO^+ + N_2$$
$$k = 0.7 \times 10^{-10} \text{ cm}^3 \text{ molecule}^{-1} \text{ s}^{-1} \text{ [19]} \qquad (39)$$
$$k = 1.2 \times 10^{-10} \text{ cm}^3 \text{ molecule}^{-1} \text{ s}^{-1} \text{ [22a]}$$

$$PtO^+ + N_2O \rightarrow Pt(O)_2^+ + N_2$$
$$k = 1.9 \times 10^{-10} \text{ cm}^3 \text{ molecule}^{-1} \text{ s}^{-1} \text{ [19]} \qquad (40)$$
$$k = 6.6 \times 10^{-10} \text{ cm}^3 \text{ molecule}^{-1} \text{ s}^{-1} \text{ [22a]}$$

$$Pt(O)_2^+ + CO \rightarrow PtO^+ + CO_2$$
$$k = 6.6 \times 10^{-10} \text{ cm}^3 \text{ molecule}^{-1} \text{ s}^{-1} \text{ [19]} \qquad (41)$$

$$PtO^+ + CO \rightarrow Pt^+ + CO_2$$
$$k = 6.4 \times 10^{-10} \text{ cm}^3 \text{ molecule}^{-1} \text{ s}^{-1} \text{ [19]} \qquad (42)$$

Clearly, both Pt⁺ and PtO⁺ can serve as catalysts in the reduction of N_2O by CO. The data given in Figure 4 convincingly demonstrate that the two cycles are coupled: quasistationary intensities of Pt⁺, PtO⁺, and $Pt(O)_2^+$ are obtained upon treating $Pt(O)_2^+$ with a mixture of CO and N_2O; within experimental error, identical stationary intensities of these ions evolve when starting from Pt⁺ and PtO⁺, respectively. Hence, the combination of Equations (39)–(42) generates a sequence in which gaseous platinum species effectively catalyze the oxidation of CO by N_2O [Eq. (43)]. Although this reaction is very exothermic, $\Delta_r H = -82.3$ kcal mol⁻¹, it does not proceed at all at ambient and elevated temperatures without a catalyst. Turnover numbers for the Pt⁺-mediated gas-phase oxidation of CO range from 80 to
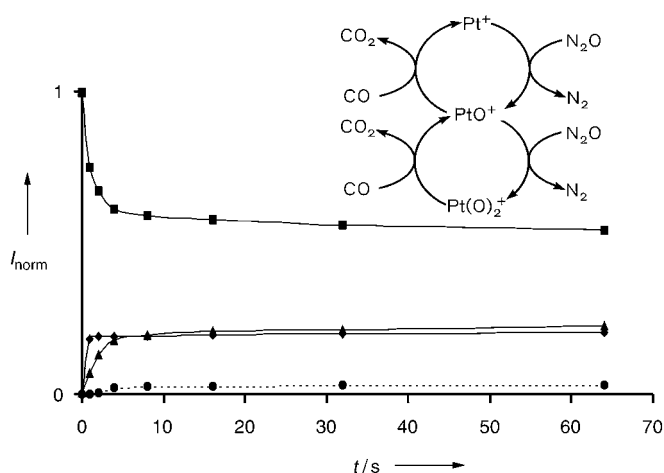
Figure 4. Temporal intensity profiles of $Pt(O)_2^+$ (■), PtO⁺ (◆), Pt⁺ (▲), and the sum of all side reaction products (●) when treating mass-selected $Pt(O)_2^+$ with a ca. 10:1 mixture of N_2O and CO (total pressure in the FTICR experiment 10^{-7} mbar). The inset shows the coupled catalytic cycles involved (adapted from ref. [19]).

300, and they are basically only limited by side reactions of the powerful oxidants PtO_n^+ ($n = 1, 2$) when they come into contact with residual hydrocarbon gas.[19]

$$2 CO + 2 N_2O \rightarrow 2 CO_2 + 2 N_2 \qquad (43)$$

Recent ICP/SIFT experiments have shown that a series of metal dioxide and higher metal oxide cations can be generated at room temperature from N_2O. For example, a second O-atom transfer was observed with the Group 4–6 transition-metal ions (except Mo⁺) as well as the third period ions Re⁺, Os⁺, Ir⁺, and Pt⁺. The atomic ions W⁺, Os⁺, and Ir⁺ form trioxides in sequential processes, and even the tetroxide OsO_4^+ can be generated from Os⁺ and N_2O.[22a] Only the higher oxides of Ir⁺ and Os⁺ have so far been treated with CO in the ICP/SIFT experiments, and these are sequentially reduced and revert back to the bare metal cation.[9,21] The reaction efficiencies of many of these O-atom transfer processes do not often correlate with the thermochemistry of the respective transformations, and quite likely this is because of the existence of spin barriers.[21,24,25]
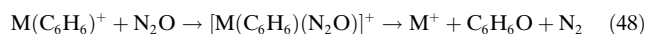
3. Bond-Activation Catalysis

The concept of catalysis through bond activation in gas-phase processes refers to situations in which the ion catalyst in, for example, oxidation reactions, does not completely abstract an oxygen atom from the terminal oxidant; rather, the catalyst simply activates a relevant part of the reagent sufficiently and transfers the reactive fragment to a second molecule trapped in the coordination sphere of the metal ion. As a consequence, significant rate enhancement often results. Three examples from different areas will be used to illustrate this concept.

The first such catalysis was demonstrated for atomic alkali-metal ions in a flowing afterglow apparatus over a large

temperature region.[52] To this end, the mass-selected cation M^+ (Li^+, Na^+, K^+) is solvated with O_3 upstream of the flow tube and allowed to react with the reductant (NO, CO, SO_2) downstream over the temperature range (125–280 K) determined by the bond energy of the alkali-metal–ozone cluster formed according to Equation (44). Although the rate constants for the association of O_3 and the reactions of the $M(O_3)^+$ complex with the substrates NO, CO, and SO_2 [Eq. (45) for the reductant NO] are not faster than 10% of the gas kinetic collision value, the measured rate constants are orders of magnitude larger than the *direct* gas-phase reaction between these neutral species [Eq. (46)] in the absence of the ions. Clearly, the alkali-metal cations M^+ act as genuine catalysts even though no covalent bond is formed between them and the two neutral molecules at any stage of the reaction.

$$O_3 + M^+ \rightarrow M(O_3)^+ \tag{44}$$

$$M(O_3)^+ + NO \rightarrow M^+ + O_2 + NO_2 \tag{45}$$

$$O_3 + NO \rightarrow O_2 + NO_2 \tag{46}$$
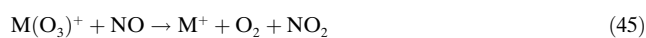
Metal ions have also been found to activate larger molecules so that they undergo chemical reactions. Thus, the gas-phase catalytic oxidation of benzene through Reactions (47) and (48) has been observed by FTICR to be catalyzed by $M^+ = Co^+$, Cr^+, and Mn^+.[38] This process is particularly interesting in the sense that it mimics heterogeneous catalysis (this will be discussed in more detail in Sections 5 and 6 for cluster-mediated reactions): In the first step, benzene coordinates to a bare M^+ ion to afford the corresponding $M(C_6H_6)^+$ species, which in the case of $M^+ = Co^+$ is formed at the collision rate; in the next step [Eq. (48)], the oxidant N_2O also coordinates to and gets activated by the metal ion to yield $M(N_2)(C_6H_6O)^+$. The high exothermicity of Reaction (49) ($\Delta_rH = -62.4$ kcal mol^{-1}) leads to evaporation of the two ligands and thus regenerates the active catalyst. The turnover number for the Co^+-catalyzed hydroxylation of benzene is 18, and is limited mostly by the formation of sandwich complexes $M(C_6H_6)_2^+$.[38]

$$C_6H_6 + M^+ \rightarrow M(C_6H_6)^+ \tag{47}$$

$$M(C_6H_6)^+ + N_2O \rightarrow [M(C_6H_6)(N_2O)]^+ \rightarrow M^+ + C_6H_6O + N_2 \tag{48}$$

$$C_6H_6 + N_2O \rightarrow C_6H_5OH + N_2 \tag{49}$$

The metal-cation mediated oxidation of benzene by molecular oxygen[53–55] has also been investigated in the gas phase, in this case by using ICP/SIFT mass spectrometry.[56] Attachment of the benzene molecule to certain metal cations activates it[57–59] sufficiently to bring about the spin-forbidden oxidation by O_2.[25] The catalytic sequence given by Reactions (47), (50), and (51) was observed for the transition-metal ions $M^+ = Cr^+$, Fe^+, and Co^+, with the crucial oxidation in Equation (50) proceeding at 30, 15, and 20% of the collision rate. While the neutral product of the oxidation is

not known, it has been suggested to be catechol, the formation of which corresponds to the most exothermic reaction pathway ($\Delta_rH = -84.8$ kcal mol^{-1}).[55h] It is interesting to recall that catechol is a major metabolite generated by the catalytic oxidation of benzene by an iron-containing dioxygenase metalloenzyme.[60]

$$M(C_6H_6)^+ + O_2 \rightarrow M^+ + C_6H_6O_2 \tag{50}$$

$$C_6H_6 + O_2 \rightarrow C_6H_4(OH)_2 \tag{51}$$
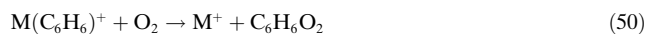
When one of the neutral products remains attached to the ion catalyst, a third reaction is needed to complete the cycle, as illustrated by Reactions (52)–(55) for the oxidation of molecular hydrogen to water by oxygen. For $M^+ = Pt^+$, the reaction sequence constitutes a gas-phase variant of the famous Döbereiner lighter.[61]

$$O_2 + M^+ \rightarrow M(O)_2^+ \tag{52}$$

$$M(O)_2^+ + H_2 \rightarrow MO^+ + H_2O \tag{53}$$

$$MO^+ + H_2 \rightarrow M^+ + H_2O \tag{54}$$

$$2\,H_2 + O_2 \rightarrow 2\,H_2O \tag{55}$$

Kinetic[19,55h] and thermochemical[50,51] data for the reactions of $M^+ = Pt^+$ have been determined by using various techniques. The effective bimolecular rate coefficient for the reaction between Pt^+ and O_2 to generate a high-valent Pt^V dioxide $Pt(O)_2^+$ has been measured at room temperature by ICP/SIFT tandem mass spectrometry to be $k_{52} = 1.6 \times 10^{-13}$ cm^3 molecule^{-1} s^{-1} in He at 0.35 Torr.[55h] The reaction of $Pt(O)_2^+$ with hydrogen proceeds with $k_{53} = 9.1 \times 10^{-11}$ cm^3 molecule^{-1} s^{-1}, and the final O-atom transfer which regenerates the Pt catalyst has a rate coefficient of $k_{54} = 5.0 \times 10^{-10}$ cm^3 molecule^{-1} s^{-1}; both values were determined by FTICR measurements.[19] A similar sequence is observed when D_2 is used instead of H_2, and the intermolecular kinetic isotope effect is minor (ca. 1.3). Thus, factors other than the mere activation of the hydrogen–hydrogen bond contribute to the rate determining step of the catalytic cycle depicted in Scheme 5.
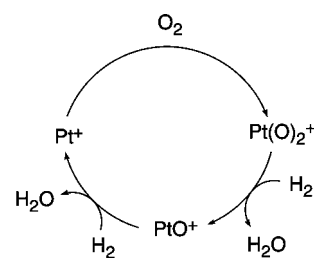

Scheme 5. Catalytic oxidation of H_2 by molecular oxygen, mediated by atomic Pt^+.

4. Metal-Mediated Coupling Processes

4.1. Formation of Carbon–Carbon Bonds

Cyclooligomerizations of unsaturated hydrocarbons are versatile reactions for the synthesis of organic systems, in particular aromatic compounds.[62] Although these reactions are quite exothermic, they are usually hampered by large kinetic barriers if non-activated hydrocarbons are involved.[62f] Transition metals have been found to facilitate these reactions in the condensed phase,[62a–d] and mass-spectrometric studies have revealed that certain "bare" transition-metal cations M$^+$ also affect the cyclization reactions of unsaturated hydrocarbons in the gas phase.[63] The cyclization is often coupled with activation of the C–H bond, and as a consequence M$^+$-mediated cyclization reactions in the gas phase are accompanied by dehydrogenation steps to eventually form quite stable aromatic complexes with M$^+$. The most classical example of the stepwise route[64] is the gas-phase trimerization of ethene by atomic W$^+$,[65] U$^+$,[66] or the Fe$_4^+$ cluster.[67]
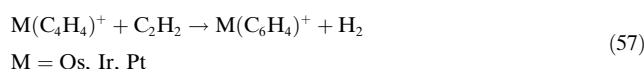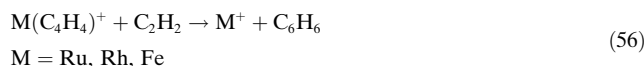
As depicted in Scheme 6, the sequence commences with the formation of a cationic metal–ethyne complex by dehydrogenation of C$_2$H$_4$. In the next, and often rate-
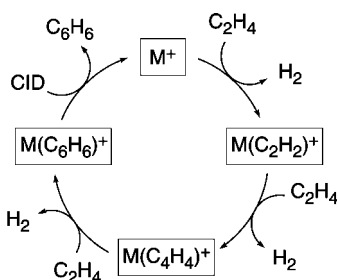
Scheme 6. Dehydrogenative oligomerization of C$_2$H$_4$ and formation of benzene by consecutive gas-phase ion–molecule reactions (adapted from ref. [67]).
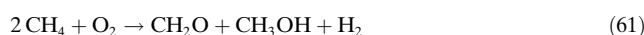
determining step, the ethyne complex undergoes dehydrogenation of a further ethene molecule to yield M(C$_4$H$_4$)$^+$; for some metal cations, for example, U$^+$, there is experimental evidence that this complex already contains a C$_4$ unit rather than two separate C$_2$H$_2$ ligands.[66] The third addition of C$_2$H$_4$ results in the formation of benzene complexes through loss of molecular hydrogen. Although the latter reaction step is very exothermic, the heat of reaction liberated is usually not sufficient to overcome the large bond dissociation energy of M$^+$-C$_6$H$_6$ to release benzene;[58, 68] as a consequence, regeneration of the active catalyst M$^+$ is not observed under thermal conditions. This is only achieved by detaching the benzene ligand from the metal center by, for example, collision-induced dissociation;[65–67] for M$^+$ = Fe$_4^+$, this requires approximately 75 kcal mol^{-1}.[67] Of course, in a "perfect" catalytic system the catalyst should be regenerated in the reaction system without additional supply of energy. This is conveniently achieved in gas-phase experiments by employing "high-energy" reactants.[64, 69a] For example, substituting ethyne for ethene as a reactant increases the exothermicity of the final

step [Eq. (56)] by approximately the heat of dehydrogenation of ethene to ethyne, that is, 42 kcal mol^{-1}. As this additional reaction energy is stored completely in the reactive complex, detachment is possible, and has been observed for M$^+$ = Ru$^+$, Rh$^+$, and Fe$^+$, with modest turnover numbers. The metal ions M$^+$ = Os$^+$, Ir$^+$, and Pt$^+$ use the extra energy to activate C–H bonds in the benzene ring and to release H$_2$ [Eq. (57)] rather than detach C$_6$H$_4$. The C$_4$H$_4$ complexes of Co$^+$ and Ni$^+$ were not found to react efficiently with C$_2$H$_2$ at a measurable rate.[64, 69b]

$$M(C_4H_4)^+ + C_2H_2 \rightarrow M^+ + C_6H_6$$
$$M = Ru, Rh, Fe$$

(56)

$$M(C_4H_4)^+ + C_2H_2 \rightarrow M(C_6H_4)^+ + H_2$$
$$M = Os, Ir, Pt$$

(57)

4.2. Formation of Carbon–Heteroatom Bonds

Bond activation and reaction coupling play a key role in the partial oxidation of methane by molecular oxygen and can be catalyzed by either Pt$^+$ or PtO$^+$.[70] The Pt$^+$-catalyzed part of the cycle involves the combination of bond activation and O-atom transport [Eqs. (58)–(61)], and leads to formaldehyde and methanol.

$$CH_4 + Pt^+ \rightarrow Pt(CH_2)^+ + H_2$$

(58)

$$Pt(CH_2)^+ + O_2 \rightarrow PtO^+ + CH_2O$$

(59)

$$PtO^+ + CH_4 \rightarrow Pt^+ + CH_3OH$$

(60)

$$2\,CH_4 + O_2 \rightarrow CH_2O + CH_3OH + H_2$$

(61)

However, Reaction (59) regenerates 70% of the atomic Pt$^+$ immediately along with CH$_2$O$_2$ (possibly formic acid), and Reaction (60) leads to 30% of the by-product Pt(CH$_2$)$^+$, which reacts further with O$_2$ to regenerate PtO$^+$. A catalytic cycle with a turnover number of about six results, which actually involves a coupling of two catalytic cycles that form an integral part of the third cycle given by Equations (58)–(60) (Scheme 7). All these reaction pathways have been
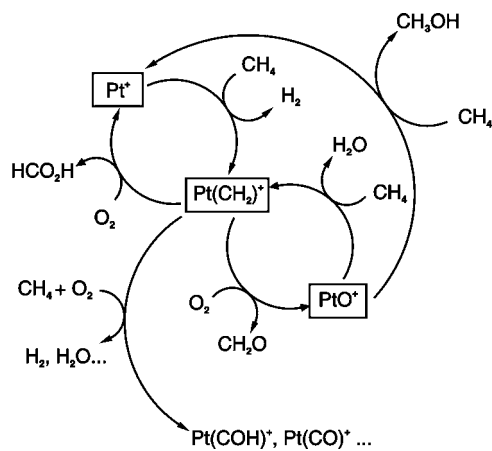
Scheme 7. Pt$^+$-catalyzed oxidation of methane by molecular oxygen (adapted from ref. [70]).

followed in detail by FTICR measurements of the various reaction kinetics, and insight into the intriguing mechanistic aspects of this complex reaction sequence was provided by electronic structure calculations which included scalar relativistic and spin-orbit effects.[71]

The platinum–carbene cation produced from methane [Eq. (58)] can also bring about the conversion of CH_4 into CO in a sequence of exothermic dehydrogenation reactions with H_2O, thus conceptually constituting a gas-phase model for a Pt^+-mediated water-gas reaction [Eq. (62)].[72] However, closing the catalytic cycle depicted in Scheme 8 by detaching
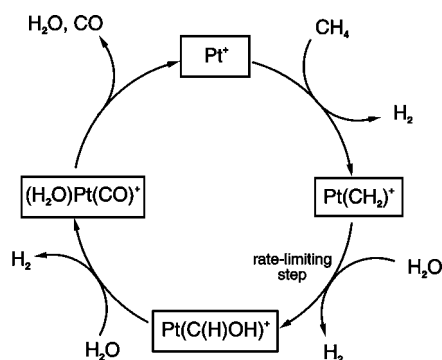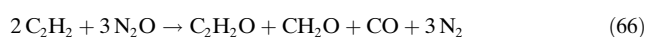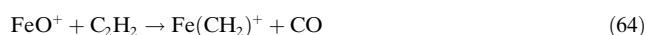

Scheme 8. Gas-phase model for a Pt^+-mediated water-gas reaction [Equation (62); adapted from ref. [72]].

the final ligands CO and H_2O from the Pt^+ catalysts requires about 102 kcal mol^{-1}. This situation is, therefore, analogous to many systems in heterogeneous catalysis, where product release from the catalytic center and regeneration of the latter is achieved by heating.

$$CH_4 + H_2O \rightarrow CO + 3 H_2 \qquad (62)$$

An interesting example of the combination of two- and three-step catalysis is the Fe^+-mediated oxidation of acetylene by N_2O.[16] The O-atom transport in Reaction (11 b) first generates FeO^+, which acts as a "monooxygenase" for the oxidation of the hydrocarbon and the positive charge of the intermediate FeO^+ leads to rate enhancement. The oxidation of acetylene itself occurs by two pathways (Reactions (63) and (64)), with an estimated branching ratio of 1/1. The production of Fe^+, according to Equation (63) and from the reaction of $Fe(CH_2)^+$ with N_2O, Equation (65), completes the three-step catalytic cycle in which formaldehyde and CO are formed according to Equation (66).

$$2 N_2O + 2 Fe^+ \rightarrow 2 FeO^+ + 2 N_2 \qquad (11b)$$

$$FeO^+ + C_2H_2 \rightarrow Fe^+ + C_2H_2O \qquad (63)$$

$$FeO^+ + C_2H_2 \rightarrow Fe(CH_2)^+ + CO \qquad (64)$$

$$Fe(CH_2)^+ + N_2O \rightarrow Fe^+ + N_2 + CH_2O \qquad (65)$$

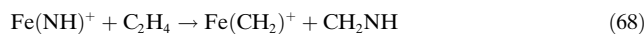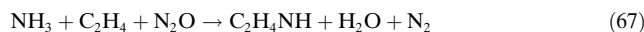$$2 C_2H_2 + 3 N_2O \rightarrow C_2H_2O + CH_2O + CO + 3 N_2 \qquad (66)$$

Catalytic formation of a C–N bond in the gas phase can occur by transfer of a NH group from a metal center to hydrocarbon substrates. Scheme 9 shows an example of the
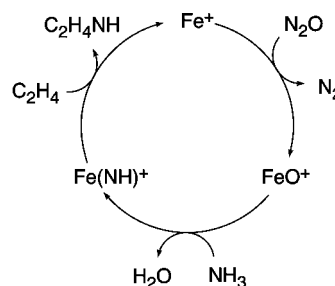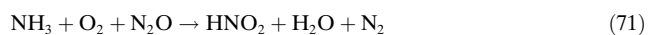

Scheme 9. Catalytic cycle illustrating the dehydrogenative C–N coupling between C_2H_4 and NH_3 (adapted from ref. [73]).

Fe^+-mediated C–N coupling reaction with ammonia and ethene [Eq. (67)]. Here bond activation is preceded by O-atom transport and followed by NH delivery to result in the formation of a C–N bond. However, in this crucial step only 38% of the reactive collisions between $Fe(NH)^+$ and C_2H_4 regenerate the Fe^+ catalyst.[73] Other ionic products are often formed, such as $Fe(NH_3)^+$ (16%) and $Fe(HNC)^+$ (15%); both may, however, also perpetuate the catalytic cycle if they react with N_2O to produce FeO^+. These scenarios have not yet been tested. Equation (68) is another product pathway (19%) that also leads to formation of a C–N bond, but it is not catalytic since the active catalyst (or a precatalyst) is not directly regenerated.[73]

$$NH_3 + C_2H_4 + N_2O \rightarrow C_2H_4NH + H_2O + N_2 \qquad (67)$$

$$Fe(NH)^+ + C_2H_4 \rightarrow Fe(CH_2)^+ + CH_2NH \qquad (68)$$

The physical properties and the chemistry of $Fe(NH)^+$ have since been studied in considerable detail by both theory and experiment.[74] The relatively low affinity of the "naked" imine NH group for Fe^+ of about 70 kcal mol^{-1} makes $Fe(NH)^+$ a strong imine donor. Indeed, gas-phase experiments have shown a propensity for $Fe(NH)^+$ to react with H_2 to form NH_3, with O_2 to produce HNO_2, with alkanes to form alkyl amines, with benzene to form aniline, and with toluene to produce benzylidenamine. All of these transformations become catalytic when coupled to the production of $Fe(NH)^+$ by Reactions (11 c), (69), and (70), since they regenerate Fe^+. This has been demonstrated for the catalytic oxidation of NH_3 to HNO_2 [Eq. (71)].

$$N_2O + Fe^+ \rightarrow FeO^+ + N_2 \qquad (11c)$$

$$FeO^+ + NH_3 \rightarrow Fe(NH)^+ + H_2O \qquad (69)$$

$$Fe(NH)^+ + O_2 \rightarrow Fe^+ + HNO_2 \qquad (70)$$

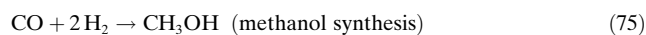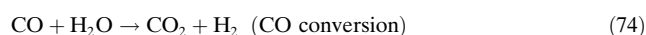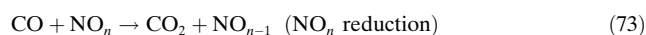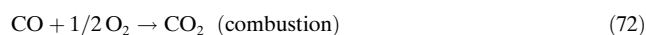$$NH_3 + O_2 + N_2O \rightarrow HNO_2 + H_2O + N_2 \qquad (71)$$

The ability to transfer NH groups can be extended to other cationic $M(NH)^+$ complexes, but may be more limited

depending on the magnitude of the M^+–NH binding energy $D(M^+$–NH). For example, $D(Y^+$–NH) has a reported lower limit of 101 kcal mol^{-1}, and this is reflected in its chemistry with alkenes, for example, which does not show any reaction pathways that regenerate Y^+ under thermal conditions.[75]

5. Toward Heterogeneous Catalysis: Gas-Phase Catalysis with Cluster Ions

The adsorption of CO on gold has been cited[76a] as the most extensively investigated chemisorption process involving gold. In spite of the inertness of metallic gold,[76] there has been recent interest worldwide in the unique activity of gold-based catalysts that facilitate numerous oxygen-atom transfer reactions at reduced temperatures and with moisture tolerance because of the observation that the activity depends critically on the size of the deposited clusters (as well as the nature of the support).[76a,77] Among these processes are a class of C_1 transformations which are of particular scientific and technical importance [Eq. (72)–(75)].

$$CO + 1/2\,O_2 \rightarrow CO_2 \quad \text{(combustion)} \tag{72}$$

$$CO + NO_n \rightarrow CO_2 + NO_{n-1} \quad \text{(NO}_n \text{ reduction)} \tag{73}$$

$$CO + H_2O \rightarrow CO_2 + H_2 \quad \text{(CO conversion)} \tag{74}$$

$$CO + 2\,H_2 \rightarrow CH_3OH \quad \text{(methanol synthesis)} \tag{75}$$

Since the catalytic activity correlates with the degree of dispersion, experiments to determine the size-dependence of finite, mass-selected gas-phase clusters were carried out.[5d,i,78,79] It was concluded on the basis of numerous studies[80] that the interplay between cluster physics and surface chemistry is a promising strategy to uncover "mechanisms of elementary steps in nanocatalysis".[81] In this Review we focus on those systems in which a full thermal catalytic cycle involving gas-phase metal clusters has been demonstrated. In these cases a "full thermal catalytic cycle" means a reaction in which one starts with a bare, mass-selected metal cluster, reactant molecules are adsorbed, then the reaction product is released to regenerate the intact cluster—all at thermal energies. Two systems will be described in detail, and both deal with the catalysis of Reaction (72) by *anionic* Pt and Au clusters. The emphasis is on negatively charged clusters, as it transpired that the metallic clusters are immobilized at surface oxide vacancies in surface reactions. These defects comprise localized electrons that can be transferred to the highly electronegative clusters bound at those sites,[77d] thus permitting electron-transfer processes with adsorbed reactants, for example, with the formation of highly reactive O_2 species.

Guided ion beam mass spectrometry has been used to demonstrate that platinum cluster anions Pt_n^- ($n = 3$–7) efficiently catalyze the oxidation of CO to CO_2 by N_2O or O_2. The reactions are exothermic and occur at approximately room temperature with no appreciable activation barrier (< 1 kcal mol^{-1} at 300 K).[5d,82a] Two catalytic cycles (a and b) were identified (Scheme 10).
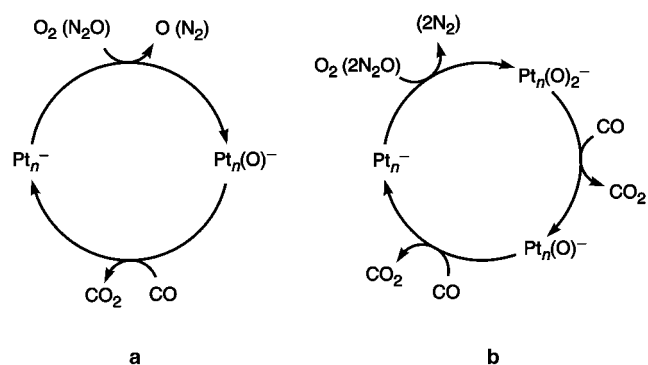

Scheme 10. Catalytic cycles observed for the oxidation of CO to CO_2 by N_2O or O_2 using Pt_n^- cluster anions (adapted from ref. [5d]).

The reaction efficiencies for the $CO \rightarrow CO_2$ conversion exceed 40% for $n \geqq 4$, so only a few collisions would be required for complete conversion. These high efficiencies at near room temperatures imply that the gas-phase Pt clusters are better catalysts than the supported catalysts used in current technology for automobile catalytic converters, which need to be heated to high temperatures;[83] temperatures of 400–500 K are typically required for the oxidation of CO on platinum surfaces.[84] The high reactivity of the gas-phase clusters may be attributable to their small size, which ensures that the metal atoms are all exposed on the surface of the cluster and are coordinatively unsaturated ("dangling bonds"). In addition, the negative charge certainly helps in the activation of molecular oxygen; the sequential oxygen-atom transfer shown in Scheme 10b evidences the presence of adsorbed atomic oxygen on the cluster surface.

The extraordinary role that supported gold clusters play in the oxidation of CO[76,77,80,81] has recently stimulated a number of computational and experimental gas-phase studies of reactions catalyzed by Au_n^-.[85] For example, efficient generation of CO_2 from CO and O_2 at room temperature has been achieved with anionic gold clusters serving as catalysts, and remarkable cooperative effects as well as size-dependent even/odd reactivity patterns were observed.[85b] O_2 adsorbs as a one-electron acceptor on Au_n clusters ($n = 4$–20),[80c,85b] with even-numbered clusters showing varying reactivity toward the adsorption of O_2, while odd-numbered clusters are unreactive. CO exhibits a highly size-dependent reactivity for $n = 4$–19, but no adsorption occurs at room temperature for $n = 2,3$. Remarkable effects have been noted when the gold clusters are exposed to both reactants, either simultaneously or sequentially. Although the same rules pertaining to individual O_2 or CO adsorption continue to apply, the preadsorption of one reactant on a cluster may lead to the increased reactivity of the cluster to the other reactant. Thus, rather than competitive coadsorption, the rare phenomenon of cooperative coadsorption is operative here. Experiments with mass-selected Au_6^- have demonstrated that this "cooperative coadsorption" gives rise to the evaporation of CO_2, thus closing the catalytic cycles by regenerating Au_6^- (Scheme 11).[85b]

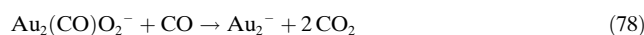A possible explanation for this enhancement of coadsorption activity is that the first adsorbate affects the
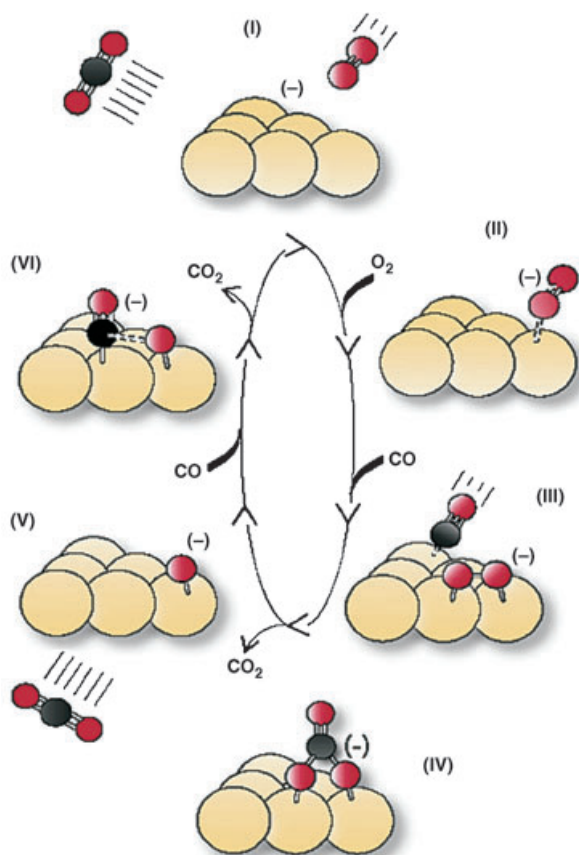
Scheme 11. Catalytic oxidations of CO to CO_2 in the presence of O_2 catalyzed by the cluster anion Au_6^- (Au yellow, C black, O red). The free Au_6^- ion in its calculated equilibrium structure (I) adsorbs O_2 in its superoxide form (II); subsequent coadsorption of CO may initially form an $Au_6CO_3^-$ species (III), which rearranges to the stable CO_3^- adsorbate (IV); elimination of CO_2 yields the Au_6O^- form (V); adsorption of a second CO yields the $Au_6CO_2^-$ species (VI), from which a second CO_2 molecule may be released and return the Au_6^- catalyst—for the sake of clarity, the Au_6^- structure is depicted as retaining the same structure throughout (adapted from ref. [85b]).

electronic structure of the cluster, thus causing it to appear electronically different to the second approaching molecule. This proposal was suggested in a recent theoretical study[85a] for the $Au_2^-/CO/O_2$ system. Accordingly, CO binds much more tightly to neutral Au_2 than to Au_2^- (1.60 versus 0.96 eV). Consequently, an Au cluster anion with a preadsorbed O_2 molecule will appear to be neutral to the approaching CO molecule because of the charge transfer that takes place from the Au_n^- cluster to the O_2 adsorbate. The analogy to the surface-catalyzed oxidation of CO becomes clear in that the excess electron (in the anionic cluster) is necessary for the reaction to occur, and the *neutral* supported clusters acquire the electron by charge transfer from the surface. A turnover frequency of approximately $100\,CO_2$ per Au atom per second has been estimated[85b] for the reaction catalyzed by Au_n^-, for $n = 10$. This efficiency is two(!) orders of magnitude greater than that seen for commercial gold catalysts.

A full catalytic cycle for Reaction (72) had been predicted theoretically for the free Au_2^- cluster,[85a] and this has been verified recently by experiments.[85c] Temperature-dependent

ion-trap mass spectrometry in combination with ab initio simulations has revealed many details of this process. Remarkably, a metastable intermediate with the elemental composition $Au_2CO_3^-$ was observed at low temperatures. For this intermediate, theory proposes two alternative structures, which correspond to digold carbonate or peroxyformate; both of these structures may serve as precursors for the formation of CO_2. Detailed kinetic studies revealed that O_2 adsorption precedes the adsorption of CO in the catalytic cycle. Furthermore, for the kinetic cycle defined by Equations (76)–(78), the steps (76) and (77) proceed without an energy barrier; in contrast, reaction (78) is associated with a small barrier. The turnover frequency amounts to $0.5\,CO_2$ molecules per gold cluster per second at room temperature. This value is on the same order of magnitude as that for the catalytic activity of oxide-supported gold cluster particles with a size of a few nanometers.[77b,c]

$$Au_2^- + O_2 \rightarrow Au_2O_2^- \tag{76}$$

$$Au_2O_2^- + CO \rightleftharpoons Au_2(CO)O_2^- \tag{77}$$

$$Au_2(CO)O_2^- + CO \rightarrow Au_2^- + 2\,CO_2 \tag{78}$$

Two basic mechanistic scenarios were explored for the formation of intermediate $Au_2CO_3^-$ (structure A in Figure 5
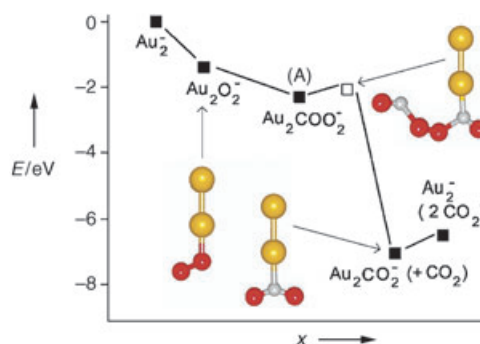
Figure 5. Energetics of the ER mechanism of the reaction, where the peroxyformate-like species $Au_2COO_2^-$ (configuration A, Au yellow, C gray, O red) is the metastable intermediate state. □ denotes the reaction barrier connecting the peroxyformate-like state with the $Au_2CO_2^- + CO_2$ products, and the corresponding transition-state configuration is shown at the top right. The last step of the reaction is desorption of CO_2. The initial energy level at zero corresponds to the sum of the total energies of all the reactants: $Au_2^- + O_2 + 2\,CO$ (adapted from ref. [85c]).

and structure B in Figure 6), that is, the Langmuir–Hinshelwood (LH) and the Eley–Rideal (ER) mechanisms, and it is only the latter pathway which is compatible with the experimental findings. As demonstrated by Figures 5 and 6, all intermediates and transition structures pertinent to the Au_2^--mediated oxidation of CO to CO_2 by molecular oxygen are located energetically well below the entrance channel. Consequently, a full catalytic cycle—even at low temperature—is possible, and this is born out experimentally.[85c]

Even *atomic* Au^- is capable of bringing about efficient catalytic oxidation of CO by O_2, as demonstrated very
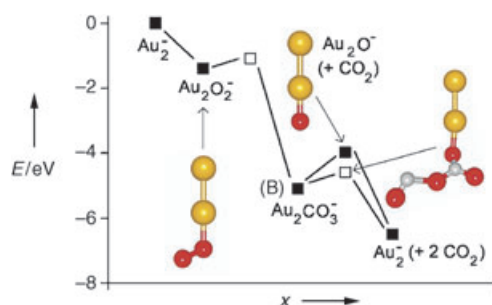
Figure 6. Energetics of the ER mechanism of the reaction in which the carbonate species Au$_2$CO$_3$$^-$ (configuration B; Au yellow, C gray, O red) is the metastable intermediate state. □ denotes the reaction barriers. The first reaction barrier is associated with the insertion of CO into the O–O bond of Au$_2$O$_2$$^-$, thus leading to the formation of Au$_2$CO$_3$$^-$. Two reaction paths are shown on the right: One path involves thermal dissociation of the carbonate to produce Au$_2$O$^-$ which then reacts with CO(g) to release another CO$_2$ molecule, while the other path proceeds through an ER reaction of the carbonate with CO(g) and results in the formation of two CO$_2$ molecules. The latter route involves a barrier of 0.5 eV, and the corresponding transition-state configuration is shown on the right (adapted from ref. [85c]).

recently in a combined experimental/computational study.[85d] Although both AuO$^-$ and AuO$_3$$^-$ (generated from Au$^-$ and O$_2$ in a fast-flow reactor) bring about the oxidation of CO, the reaction of AuO$_2$$^-$ with CO proceeds at an extremely low rate as a result of a relatively high energy barrier involved in the formation of the complex and the existence of spin barriers arising from the inefficient crossings between the singlet and triplet potential energy surfaces. In contrast, the reaction of the two other much more reactive AuO$_n$$^-$ oxides ($n = 1, 3$) with CO is not impeded by spin restrictions.[85d]

6. Processes Mediated by Metal-Oxide Clusters: Redox versus Nonredox Reactivities

Metal oxides are able to catalyze numerous processes in both the condensed[7c,j,k,30c,86] and the gas phase.[5a,e,43] Here, we will briefly discuss three examples which may serve to define the scope and limitations of a gas-phase approach in the context of cluster-mediated oxidation catalysis. Two gas-phase cycles (Scheme 12a and b) were detected by multistage mass-spectrometry experiments[87] for the two-electron oxidation of primary and secondary alcohols, and a binuclear anionic dimolybdate center [Mo$_2$O$_6$(OCHR$_2$)]$^-$ acts as the central intermediate in both these cycles. Three steps have been characterized: 1) condensation of [Mo$_2$O$_6$(OH)]$^-$ with the alcohol R$_2$CHOH and elimination of water to produce the alkoxo-bound cluster; 2) oxidation of the alkoxo ligand and its liberation as an aldehyde or a ketone in a step which is rate-limiting and requires the supply of external energy through collisional activation; 3) regeneration of the catalyst is achieved by oxidation with nitromethane. The second cycle is similar, but differs in the order of the reaction with the alcohol and the terminal oxidant nitromethane (see Scheme 12 for R$_2$CHOH=CH$_3$OH).[87]
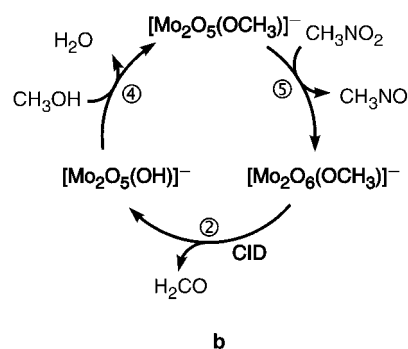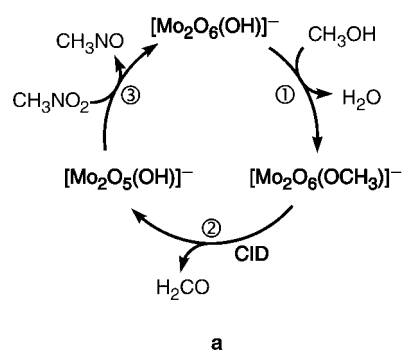
Scheme 12. Gas-phase catalytic cycles for the oxidation of methanol to formaldehyde. The second reaction step links [Mo$_2$O$_6$(OCH$_3$)]$^-$ and [Mo$_2$O$_5$(OH)]$^-$ and appears in both cycles. The two cycles a and b differ in the sequence of reaction with CH$_3$NO$_2$ and CH$_3$OH (adapted from ref. [87]).

The role of the binuclear metal center was assessed by examination of the relative reactivities of the mononuclear [MO$_3$(OH)]$^-$ and binuclear [M$_2$O$_6$(OH)]$^-$ complexes (M = Cr, Mo, W). The molybdenum and tungsten binuclear centers (M = Mo, W) were reactive toward alcohol but the chromium complex was not; this finding is consistent with the order of basicity of the hydroxo ligand in these anionic complexes. However, the tungsten center [W$_2$O$_6$(OCHR$_2$)]$^-$ prefers a nonredox elimination of an alkene rather than oxidation of the alkoxo ligand to form an aldehyde or a ketone. This observation is consistent with the oxidizing power of the anions. Interestingly, each of the mononuclear anions [MO$_3$(OH)]$^-$ (M = Cr, Mo, W) was inert to reaction with methanol and this highlights the importance of the second MO$_3$ unit in the catalytic cycles. Clearly, only the bimolybdate center has the appropriate mix of electronic properties that allow it to participate in each of the three steps, which corresponds to the unique role of Mo^{VI} trioxide in the industrial oxidation of methanol to formaldehyde at 300–400 °C.[88]

The dinuclear manganese oxide cations Mn$_2$O$_2$$^+$ and Mn$_2$O$^+$ were generated for gas-phase dioxygen activation studies[89] and found to be potentially active as catalysts in the oxidation of alcohols and aldehydes as well as in the oxidative coupling of unsaturated hydrocarbons.[89] However, the input of external energy is essential to close the catalytic cycle for

the $Mn_2O_n^+$ ($n = 1, 2$) reactions for at least one of the steps. This can be achieved by product release by collisional activation or, preferably, by a ligand-exchange process.

Finally, a two-step gas-phase catalytic cycle for the dehydration of acetic acid to ketene was realized for mononuclear and dinuclear oxo anions $[MO_3(OH)]^-$ and $[M_2O_6(OH)]^-$ ($M = Mo$, W).[90a] Some of the mechanistic features of this metal-mediated nonredox process resemble those suggested for the dehydration of acetic acid over metal oxide and silica surfaces.[91]

7. Conclusions

This Review has demonstrated that the application of mass-spectrometric techniques to the study of elementary ion reactions has led to remarkable progress in a relatively short time in the characterization of detailed aspects of the kinetics, thermodynamics, and mechanisms of molecular transformations catalyzed by gas-phase ions. Of course, there are few natural environments, other than the earth's atmosphere, in which gas-phase ion catalysis plays a chemically important role, and practical applications of gas-phase ion catalysis are yet to be exploited (for example, perhaps in future catalytic converters).

However, there can be no doubt that what has so far been learned about ion catalysis in the gas phase is most instructive in the understanding of important fundamental aspects of practical catalysis in the condensed phase. Although the intrinsic catalytic properties of atomic ions are beginning to be well understood, much remains to be learned from future mass-spectrometric investigations about the catalytic properties of ligated ions and cluster ions. The latter will provide the necessary insights that will bridge the gap in our understanding between gas-phase reactions catalyzed by atomic ions and heterogeneous catalysis in the condensed phase—after all, ions in the gas phase provide the "single sites" that are active in surface catalysis.[62g, 92]

[1] E. Fischer, *Stahl Eisen* **1912**, *32*, 1898.

[2] D. F. Shriver, P. W. Atkins, C. H. Langford, *Inorganic Chemistry*, Oxford University Press, Oxford, **1994**, chap. 17.

[3] *Opportunities in Chemistry*, National Academy Press, Washington, DC, **1985**.

[4] a) G. A. Olah, A. Molnar, *Hydrocarbon Chemistry*, Wiley, New York, **1995**; b) A. E. Shilov, G. B. Shul'pin, *Chem. Rev.* **1997**, *97*, 2879; c) A. Sen, *Acc. Chem. Res.* **1998**, *31*, 550; d) W. D. Jones, *Science* **2000**, *287*, 1942; e) J. R. Rostrup-Nielsen, *Catal. Today* **2000**, *63*, 159; f) J. H. Lunsford, *Catal. Today* **2000**, *63*, 165; g) R. H. Crabtree, *J. Chem. Soc. Dalton Trans.* **2001**, 2437; h) A. A. Fokin, P. R. Schreiner, *Chem. Rev.* **2002**, *102*, 1551; i) J. A. Labinger, J. E. Bercaw, *Nature* **2002**, *417*, 507; j) U. Fekl, K. I. Goldberg, *Adv. Inorg. Chem.* **2003**, *54*, 259; k) C. J. Jones, D. Taube, V. R. Ziatdinov, R. A. Periana, R. J. Nielsen, J. Oxgaard, W. A. Goddard III, *Angew. Chem.* **2004**, *116*, 4726; *Angew. Chem. Int. Ed.* **2004**, *43*, 4626, and references therein; l) D. Milstein, *Pure Appl. Chem.* **2003**, *75*, 445; m) M. E. Van der Boom, D. Milstein, *Chem. Rev.* **2003**, *103*, 1759; n) U. Fekl, K. I. Goldberg, *Adv. Inorg. Chem.* **2003**, *54*, 2590.

[5] For recent reviews, see: a) D. Schröder, H. Schwarz, *Angew. Chem.* **1995**, *107*, 2126; *Angew. Chem. Int. Ed. Engl.* **1995**, *34*, 1973; b) H. Schwarz, D. Schröder, *Pure Appl. Chem.* **2000**, *72*, 2319; c) D. A. Plattner, *Int. J. Mass Spectrom.* **2001**, *207*, 125; d) K. M. Ervin, *Int. Rev. Phys. Chem.* **2001**, *20*, 127; e) K. A. Zemski, D. R. Jurtes, A. W. Castleman, Jr., *J. Phys. Chem. B* **2002**, *106*, 6136; f) U. Mazurek, H. Schwarz, *J. Chem. Soc. Chem. Commun.* **2003**, 1321; g) H. Schwarz, *Angew. Chem.* **2003**, *115*, 4580; *Angew. Chem. Int. Ed.* **2003**, *42*, 4442; h) R. A. J. O'Hair, G. N. Khairallah, *J. Cluster Sci.* **2004**, *15*, 331; i) T. Waters, R. A. J. O'Hair, *Encylopedia of Mass Spectrometry*, (Ed.: N. M. M. Nibbering), Vol. *4*, Elsevier, New York, **2005**, 604; j) P. Chen, *Angew. Chem.* **2003**, *115*, 2938; *Angew. Chem. Int. Ed.* **2003**, *42*, 2832.

[6] a) *Gaseous Ion Chemistry and Mass Spectrometry* (Ed.: J. H. Futrell), Wiley, New York, **1986**; b) K. Eller, H. Schwarz, *Chem. Rev.* **1991**, *91*, 1121; c) "Modern Mass Spectrometry": *Top. Curr. Chem.* **2003**, *225*, Springer, Berlin, **2003**; d) J. H. Gross, *Mass Spectrometry*, Springer, Berlin, **2004**.

[7] For a selection of leading references, see: a) G. Ertl in *Elementary Steps in Ammonia Synthesis. The Surface Science Approach* (Ed.: J. R. Jennings), Plenum, New. York, **1991**, p. 109; b) J. M. Thomas, R. Schlögl, *Angew. Chem.* **1994**, *106*, 316; *Angew. Chem. Int. Ed. Engl.* **1994**, *33*, 308; c) *Applied Homogeneous Catalysis with Organometallic Compounds*, Vol. *1*,2 (Eds.: B. Cornils, W. A. Herrmann), VCH, Weinheim, **1996**; d) J. M. Thomas, *Chem. Eur. J.* **1997**, *3*, 1557; e) G. Ertl, H. J. Freund, *Phys. Today* **1999**, *52*, 32; f) G. A. Somorjai, K. McKrea, *Appl. Catal. A* **2001**, *222*, 3; g) R. Noyori, T. Ohkuma, *Angew. Chem.* **2001**, *113*, 40; *Angew. Chem. Int. Ed.* **2001**, *40*, 41; h) T. M. Tonka, R. H. Grubbs, *Acc. Chem. Res.* **2001**, *34*, 18; i) G. Ertl, *J. Mol. Catal. A* **2002**, *182*/183, 5; j) A. T. Bell, *Science* **2003**, *299*, 1688; k) R. Schlögl, S. B. A. Hamid, *Angew. Chem.* **2004**, *116*, 1656; *Angew. Chem. Int. Ed.* **2004**, *43*, 1628; l) X. Zhang, X. Chen, P. Chen, *Organometallics* **2004**, *23*, 3437; m) S. S. Stahl, *Angew. Chem.* **2004**, *116*, 3480; *Angew. Chem. Int. Ed.* **2004**, *43*, 3400; n) A. Ajamian, J. L. Gleason, *Angew. Chem.* **2004**, *116*, 3842; *Angew. Chem. Int. Ed.* **2004**, *43*, 3754; for reviews with an emphasis on heterogeneous catalysis on the atomic scale, see: o) M. Boudart, *Catal. Lett.* **2000**, *65*, 1; p) G. Ertl, *Chem. Rec.* **2000**, 33; q) G. Ertl, *J. Mol. Catal. A* **2002**, *182*/183, 5; r) J. M. Thomas, C. R. A. Catlow, G. Sankar, *Chem. Commun.* **2002**, 2921; s) B. de Bruin, P. H. M. Budzelaar, A. G. Wal, *Angew. Chem.* **2004**, *116*, 4236; *Angew. Chem. Int. Ed.* **2004**, *43*, 4142; t) C. Copéret, M. Chabanas, R. P. Saint-Arromant, J.-M. Basset, *Angew. Chem.* **2003**, *115*, 164; *Angew. Chem. Int. Ed.* **2003**, *42*, 156; u) C. Hahn, *Chem. Eur. J.* **2004**, *10*, 5888; v) K. Reuter, D. Frenkel, M. Scheffler, *Phys. Rev. Lett.* **2004**, *93*, 116105-1; w) G. W. Coates, D. R. Moore, *Angew. Chem.* **2004**, *116*, 6784; *Angew. Chem. Int. Ed.* **2004**, *43*, 6618.

[8] a) *Collision Spectroscopy* (Ed.: R. G. Cooks), Plenum Press, New York, **1978**; b) K. L. Busch, G. L. Glish, S. A. McLuckey, *Mass Spectrometry/Mass Spectrometry: Techniques and Applications of Tandem Mass Spectrometry*, VCH, Weinheim, **1988**.

[9] V. Blagojevic, G. Orlova, D. K. Bohme, *J. Am. Chem. Soc.* **2005**, *127*, 3345.

[10] a) G. Bouchoux, J.-Y. Salpin, D. Leblanc, *Int. J. Mass Spectrom. Ion Processes* **1996**, *153*, 37; b) G. Bouchoux, J.-Y. Salpin, *J. Phys. Chem.* **1996**, *100*, 16555; c) M. Moomann, S. Bashir, P. J. Derrick, D. Kuck, *J. Am. Soc. Mass Spectrom.* **2000**, *11*, 544; d) G. Bouchoux, D. Leblanc, M. Sabbier, *Int. J. Mass Spectrom.* **2001**, *210/211*, 189.

[11] E. E. Ferguson, F. C. Fehsenfeld, *J. Geophys. Res.* **1968**, *73*, 6215.

[12] F. Kaufman, *Defense Nuclear Agency Reaction Rate Handbook*, DASIAC, General Electric, TEMPO, Santa Barbara, CA, **1972**, chap. 19.

[13] a) *Ion Molecule Reactions: Kinetics and Dynamics* (Ed.: J. L. Franklin), Dowden, Hutchinson and Ross, Strondsburg, PA, **1979**; b) *Gas Phase Ion Chemistry*, Vol. *1–3* (Ed.: M. T. Bowers), Academic Press, New York, **1979**; c) *Techniques for the Study of Ion-Molecule Reactions* (Eds.: J. M. Farrar, W. H. Saunders, Jr.), Wiley, New York, **1988**; d) R. Zahradnik, *Acc. Chem. Res.* **1995**, *28*, 306.

[14] J. M. C. Plane, *Chem. Rev.* **2003**, *103*, 4963, and references therein.

[15] a) V. I. Parvulescu, P. Grange, B. Oelmon, *Catal. Today* **1998**, *46*, 233, and references therein; b) R. Burch, J. P. Breen, C. F. Meunier, *Appl. Catal. B* **2002**, *39*, 283; c) for a recent review on *biological* reduction of N_2O, see: P. Chen, S. I. Gorelsky, S. Ghosh, E. I. Solomon, *Angew. Chem.* **2004**, *116*, 4224; *Angew. Chem. Int. Ed.* **2004**, *43*, 4132; d) for an ab initio analysis of catalytic NO reduction, see: Z.-P. Liu, S. J. Denkins, D. A. King, *J. Am. Chem. Soc.* **2004**, *126*, 10746; e) for first principles calculations on the oxidation of alkali metal atoms with N_2O, see: O. Tishchenko, C. Vinckier, M. T. Nguyen, *J. Phys. Chem. A* **2004**, *108*, 1268.

[16] M. M. Kappes, R. H. Staley, *J. Am. Chem. Soc.* **1981**, *103*, 1286.

[17] V. Baranov, G. Javahery, A. C. Hopkinson, D. K. Bohme, *J. Am. Chem. Soc.* **1995**, *117*, 12801.

[18] For a theoretical study of the dissociation of N_2O in reactions catalyzed by transition-metal ions, see: A. Martinez, A. Goursot, R. Castañeda, A. Corma, *J. Phys. Chem. B* **2004**, *108*, 8823.

[19] M. Brönstrup, D. Schröder, I. Kretzschmar, H. Schwarz, J. N. Harvey, *J. Am. Chem. Soc.* **2001**, *123*, 142.

[20] V. Blagojevic, M. J. Y. Jarvis, E. Flaim, G. K. Koyanagi, V. V. Lavrov, D. K. Bohme, *Angew. Chem.* **2003**, *115*, 5073; *Angew. Chem. Int. Ed.* **2003**, *42*, 4923.

[21] a) G. K. Koyanagi, V. V. Lavrov, V. I. Baranov, D. Bandura, S. D. Tanner, J. W. McLaren, D. K. Bohme, *Int. J. Mass Spectrom.* **2000**, *194*, L1; b) G. K. Koyanagi, V. I. Baranov, S. T. Tanner, D. K. Bohme, *J. Anal. At. Spectrom.* **2000**, *15*, 1207.

[22] a) V. V. Lavrov, V. Blagojevic, G. K. Koyanagi, G. Orlova, D. K. Bohme, *J. Phys. Chem. A* **2004**, *108*, 5610; b) G. K. Koyanagi, D. K. Bohme, *J. Phys. Chem. A* **2001**, *105*, 8964.

[23] T. Su, W. J. Chesnawich, *J. Chem. Phys.* **1982**, *76*, 5183.

[24] I. Kretzschmar, A. Fiedler, J. N. Harvey, D. Schröder, H. Schwarz, *J. Phys. Chem. A* **1997**, *101*, 6252.

[25] For a recent exhaustive review on the topic of "spin-forbiddeness" in ion-molecule reactions, see: H. Schwarz, *Int. J. Mass Spectrom.* **2004**, *237*, 75.

[26] a) D. E. Clemmer, Y.-M. Chen, F. A. Khan, P. B. Armentrout, *J. Phys. Chem.* **1994**, *98*, 6522; b) D. Schröder, A. Fiedler, M. F. Ryan, H. Schwarz, *J. Phys. Chem.* **1994**, *98*, 68; c) A. Fiedler, D. Schröder, S. Shaik, H. Schwarz, *J. Am. Chem. Soc.* **1994**, *116*, 19734; d) S. Shaik, D. Danovich, A. Fiedler, D. Schröder, H. Schwarz, *Helv. Chim. Acta* **1995**, *78*, 1393; e) D. Schröder, H. Schwarz, D. E. Clemmer, Y. Chen, P. B. Armentrout, V. I. Baranov, D. K. Bohme, *Int. J. Mass Spectrom. Ion Processes* **1997**, *161*, 175; f) D. Danovich, S. Shaik, *J. Am. Chem. Soc.* **1997**, *119*, 1773; g) M. Filatov, S. Shaik, *J. Phys. Chem. A* **1998**, *102*, 3835.

[27] a) R. Poli, J. N. Harvey, *Chem. Soc. Rev.* **2003**, *32*, 1; b) R. Poli, *J. Organomet. Chem.* **2004**, *689*, 4291.

[28] For a review, see: D. Schröder, S. Shaik, H. Schwarz, *Acc. Chem. Res.* **2000**, *33*, 139.

[29] A. Fiedler, J. Hrušák, W. Koch, H. Schwarz, *Chem. Phys. Lett.* **1993**, *211*, 242.

[30] a) D. Schröder, H. Schwarz, S. Shaik, *Struct. Bonding (Berlin)* **2000**, *97*, 91; b) for reviews on metal-mediated oxygen-atom transfer catalysis in solution, see: *Catalytic Asymmetric Synthesis*, 2nd ed. (Ed.: I. Ojima), Wiley-VCH, New York, **2000**; c) *Oxygenases and Model Systems* (Ed.: T. Fumabiki), Kluwer, Boston, **1997**; d) *Comprehensive Organometallic Chemistry II*, Vol. *12* (Eds.: G. Wilkinson, F. G. A. Stone, E. W. Abel, L. S. Hegedus), Pergamon, New York, **1995**.

[31] D. Schröder, H. Schwarz, *Angew. Chem.* **1990**, *102*, 1468; *Angew. Chem. Int. Ed. Engl.* **1990**, *29*, 1433.

[32] T. C. Jackson, D. B. Jacobson, B. S. Freiser, *J. Am. Chem. Soc.* **1984**, *106*, 1252.

[33] H. Kang, J. L. Beauchamp, *J. Am. Chem. Soc.* **1986**, *108*, 5663.

[34] a) A. E. Stevens, J. L. Beauchamp, *J. Am. Chem. Soc.* **1971**, *93*, 6449; b) P. B. Armentrout, J. L. Beauchamp, *J. Chem. Phys.* **1981**, *74*, 2819; c) R. Georgiadis, P. B. Armentrout, *Int. J. Mass Spectrom. Ion Processes* **1989**, *89*, 227; d) S. K. Loh, E. R. Fisher, L. Lian, R. H. Schultz, P. B. Armentrout, *J. Phys. Chem.* **1989**, *93*, 3159; e) E. R. Fisher, P. B. Armentrout, *J. Phys. Chem.* **1990**, *94*, 1674.

[35] D. Schröder, H. Schwarz, *Angew. Chem.* **1990**, *102*, 1466; *Angew. Chem. Int. Ed. Engl.* **1990**, *29*, 1431.

[36] K. K. Irikura, J. L. Beauchamp, *J. Am. Chem. Soc.* **1989**, *111*, 75.

[37] N. Ktiajsma, M. Ito, H. Fukui, Y. Moro-Oka, *J. Chem. Soc. Chem. Commun.* **1991**, *102*, and references therein.

[38] M. F. Ryan, D. Stöckigt, H. Schwarz, *J. Am. Chem. Soc.* **1994**, *116*, 9565.

[39] Y. Shiota, K. Yoshizawa, *J. Chem. Phys.* **2003**, *118*, 5872, and references therein.

[40] At thermal energies the reverse reaction $Fe(OH)^+ + CH_3 \rightarrow FeO^+ + CH_4$ takes place instead: O. Blum, D. Stöckigt, D. Schröder, H. Schwarz, *Angew. Chem.* **1992**, *104*, 637; *Angew. Chem. Int. Ed. Engl.* **1992**, *31*, 603.

[41] a) S. T. Ceyer, *Science* **1990**, *249*, 133; b) J. C. Mackie, *Catal. Rev. Sci. Eng.* **1991**, *33*, 169; c) H. Schwarz, *Angew. Chem.* **1991**, *103*, 837; *Angew. Chem. Int. Ed. Engl.* **1991**, *30*, 820; d) J. Kiwi, K. R. Thampi, M. Grätzel, P. Albers, K. Seibold, *J. Phys. Chem.* **1992**, *96*, 1344; e) Z. Zhang, X. E. Verykios, M. Baerns, *Catal. Rev. Sci. Eng.* **1993**, *35*, 169.

[42] D. Schröder, R. Wesendrup, C. A. Schalley, W. Zummack, H. Schwarz, *Helv. Chim. Acta* **1996**, *79*, 123.

[43] D. Schröder, H. Schwarz in *Essays in Contemporary Chemistry: From Molecular Structure towards Biology* (Eds.: G. Quinkert, M. V. Kisakürek), Verlag Helvetica Chimica Acta, Zürich, **2001**, p. 131.

[44] For enhancement effects of added methanol on selective CH_4 oxidations, see: Y. Teng, Y. Yamaguchi, T. Takemoto, K. Tabata, E. Suzuki, *Phys. Chem. Chem. Phys.* **2000**, *2*, 3429.

[45] a) *Organometallic Ion Chemistry* (Ed.: B. S. Freiser), Kluwer, Dordrecht, **1996**, p. 283; b) S. G. Lias, J. E. Bartmess, J. F. Liebman, J. L. Holmes, R. D. Levin, W. G. Mallard, *J. Phys. Chem. Ref. Data Suppl. 1* **1988**, *17*.

[46] A. Fiedler, D. Schröder, H. Schwarz, B. L. Tjelta, P. B. Armentrout, *J. Am. Chem. Soc.* **1996**, *118*, 5047.

[47] I. Kretzschmar, D. Schröder, H. Schwarz, unpublished results.

[48] D. Stöckigt, H. Schwarz, *Liebigs Ann.* **1995**, 429.

[49] D. Schröder, M. C. Holthausen, H. Schwarz, *J. Phys. Chem. B* **2004**, *108*, 14 407.

[50] X.-G. Zhang, P. B. Armentrout, *J. Phys. Chem. A* **2003**, *107*, 8904.

[51] X.-G. Zhang, P. B. Armentrout, *J. Phys. Chem. A* **2003**, *107*, 8915.

[52] B. R. Rowe, A. A. Viggiano, F. C. Fehsenfeld, D. W. Fakey, E. E. Ferguson, *J. Chem. Phys.* **1982**, *76*, 742.

[53] The fundamental aspects associated with the activation of molecular oxygen as well as the "stoichiometry problem" will not be addressed in detail here. For general introductions, see ref. [54], and for some examples pertinent to the content of the present review, see refs. [11,30,43,50,51,55].

[54] a) E. F. Elstner, *Der Sauerstoff*, Wissenschaftsverlag, Mannheim, **1990**; b) D. T. Sawyer, *Oxygen Chemistry*, Oxford University Press, New York, **1991**.

[55] a) R. Johnson, F. R. Castell, M. A. Biondi, *J. Chem. Phys.* **1974**, *61*, 5404; b) M. M. Kappes, R. H. Staley, *J. Phys. Chem.* **1981**, *85*, 942; c) S. Dheandhanoo, B. K. Chatterjee, R. Johnson, *J. Chem. Phys.* **1985**, *83*, 3327; d) E. R. Fisher, J. L. Elkind, D. E. Clemmer, R. Georgiadis, S. K. Loh, N. Aristov, L. S. Sunderlin, P. B. Armentrout, *J. Chem. Phys.* **1990**, *93*, 942; e) A. Fiedler, I. Kretzschmar, D. Schröder, H. Schwarz, *J. Am. Chem. Soc.* **1996**, *118*, 9941; f) R. J. Rollason, J. M. C. Plane, *J. Chem. Soc. Faraday Trans.* **1998**, *94*, 3067; g) M. K. Beyer, C. B. Berg, U. Achatz, S. Joos, G. Niedner-Schatteburg, V. E. Bondybey, *Mol. Phys.* **2001**, *99*, 699; h) G. K. Koyanagi, D. Caraiman, V. Blagojevic, D. K. Bohme, *J. Phys. Chem. A* **2002**, *106*, 4581.

[56] We note in passing that it is this very feature that has caused some interest in the role of metal-ion interactions with benzene in interstellar chemistry, in which benzene can contribute to the depletion of atomic ions and can act as a platform for catalytic gas-phase chemistry. For leading references, see ref. [57]. For a recent computational study on various aspects of the M^+/C_6H_6 interactions, see: ref. [58], and for a review on the role of π interactions with metal cations in biological systems, see: ref. [59].

[57] a) D. K. Bohme, *Chem. Rev.* **1992**, *92*, 1487; b) P. Boissel, *Astron. Astrophys.* **1994**, *285*, L33; c) F. Pirani, D. Coppelletti, M. Bartolomei, V. Aquilanti, M. Scotoni, M. Vescovi, D. Ascenzi, D, Bassi, *Phys. Rev. Lett.* **2001**, *86*, 5035.

[58] M. Diefenbach, H. Schwarz, *Encycl. Comput. Chem.* **2004**, DOI: 10.1002/0470845015.cn0091 (Aug 15, 2004)..

[59] a) D. A. Dougherty, *Science*, **1996**, *271*, 163; b) J. C. Ma, D. A. Dougherty, *Chem. Rev.* **1997**, *97*, 1303.

[60] S. Mallier-Soulier, V. Ducrocq, N. Truffant, *Can. J. Microbiol.* **1999**, *45*, 898.

[61] For a superb discussion on the intricacies in the oxidation of hydrogen on Pt(111), see: a) S. Völkening, K. Bedürftig, K. Jacobi, J. Wintterlin, G. Ertl, *Phys. Rev. Lett.* **1999**, *83*, 2672; b) C. Sachs, M. Hildebrand, S. Völkening, J. Wintterlin, G. Ertl, *Science* **2001**, *293*, 1635; c) C. Sachs, M. Hildebrand, S. Völkening, J. Wintterlin, G. Ertl, *J. Chem. Phys.* **2002**, *116*, 5759, and references therein; d) the discovery of the platinum-catalyzed oxidation of hydrogen in 1823 by Döbereiner (J. W. Döbereiner, *Schweigg. J.* **1823**, *39*, 1) prompted Berzelius to coin the term "catalysis" (J. J. Berzelius, *Iber. Chem.* **1837**, *15*, 237). For a historical account, entitled "Katalyse: Vom Stein der Weisen zu Wilhelm Ostwald", see: G. Ertl, T. Gloyna, *Z. Phys. Chem.* **2003**, *217*, 1207; e) the catalytic oxidation of hydrogen on free *neutral* platinum clusters has been reported by: M. Andersson, A. Rosén, *J. Chem. Phys.* **2002**, *117*, 7051.

[62] a) K. P. C. Vollhardt, *Angew. Chem.* **1984**, *96*, 525; *Angew. Chem. Int. Ed. Engl.* **1984**, *23*, 539; b) N. E. Shore, *Chem. Rev.* **1988**, *88*, 1081; c) M. Lautens, W. Klute, W. Tam, *Chem. Rev.* **1996**, *96*, 49; d) I. Ojima, M. Tzamaviondaki, Z. Li, R. J. Donovan, *Chem. Rev.* **1996**, *96*, 635; e) for a discussion of electron-transfer catalysis using transition-metal complexes, see: S. Hintz, A. Heidbreider, J. Mattay, *Top. Curr. Chem.* **1996**, *177*, 78; f) a

survey as well as a detailed computational analysis of the noncatalyzed trimerization of, for example, $3C_2H_2 \rightarrow C_6H_6$, can be found in: R. D. Bach, G. J. Wolber, H. B. Schlegel, *J. Am. Chem. Soc.* **1985**, *107*, 2837; g) for a recent example for C_2H_2 trimerization on single Ag, Rh, and Pd atoms supported on the MgO(001) surface, see: A. S. Wörz, K. Judai, S. Abbet, J.-M. Antonietti, U. Heiz, A. DelVitto, L. Giordano, G. Pacchioni, *Chem. Phys. Lett.* **2004**, *399*, 266; h) for ethylene polymerization mediated by oxygenated chromium cluster ions and the relationship between gas-phase reactivities of isolated clusters versus solid-state behavior, see: T. Hanmura, M. Ichihashi, T. Monoi, K. Matsuura, T. Kondow, *J. Phys. Chem. A*, **2004**, *108*, 10434.

[63] a) S. W. Buckner, T. J. MacMahon, G. D. Byrd, B. S. Freiser, *Inorg. Chem.* **1989**, *28*, 3511; b) R. Bakhtiar, J. J. Drader, D. B. Jacobson, *J. Am. Chem. Soc.* **1992** *114*, 8304.

[64] R. Wesendrup, H. Schwarz, *Organometallics* **1997**, *16*, 461

[65] C. Berg, S. Kaiser, T. Schindler, C. Kronseder, G. Niedner-Schatteburg, V. E. Bondybey, *Chem. Phys. Lett.* **1994**, *231*, 139.

[66] C. Heinemann, H. H. Cornehl, H. Schwarz, *J. Organomet. Chem.* **1995**, *501*, 201.

[67] a) P. Schnabel, M. P. Irion, K. G. Weil, *J. Phys. Chem.* **1991**, *95*, 9688; b) P. Schnabel, K. G. Weil, M. P. Irion, *Angew. Chem.* **1992**, *104*, 633; *Angew. Chem. Int. Ed. Engl.* **1992**, *31*, 636; c) O. Gehret, M. P. Irion, *Chem. Phys. Lett.* **1996**, *254*, 379..

[68] a) V. Ryzhov, R. C. Dunbar, *J. Am. Chem. Soc.* **1999**, *121*, 2259; b) for a recent review, see: L. Operti, R. Rabezzana, *Mass Spectrom. Rev.* **2003**, *22*, 407.

[69] a) For details of the gas-phase oligomerization of C_2H_2 mediated by atomic Fe$^+$ see: D. Schröder, D. Sülzle, J. Hrušák, D. K. Bohme, H. Schwarz, *Int. J. Mass Spectrom. Ion Processes* **1991**, *110*, 145; b) for an infrared spectroscopic characterization of gaseous $Ni(C_2H_2)_n{}^+$ ($n = 3$–6) complexes that provide evidence for intracluster cyclization reactions, see: R. S. Walters, T. D. Draeger, M. A. Duncan, *J. Phys. Chem. A* **2002**, *106*, 10482; c) M. A. Duncan, *Int. Rev. Phys. Chem.* **2003**, *22*, 407.

[70] R. Wesendrup, D. Schröder, H. Schwarz, *Angew. Chem.* **1994**, *106*, 1232; *Angew. Chem. Int. Ed. Engl.* **1994**, *33*, 1174.

[71] M. Pavlov, M. R. A. Blomberg, P. E. M. Siegbahn, R. Wesendrup, C. Heinemann, H. Schwarz, *J. Phys. Chem. A* **1997**, *101*, 1567, and references therein.

[72] M. Brönstrup, D. Schröder, H. Schwarz, *Organometallics* **1999**, *18*, 1939.

[73] S. W. Buckner, J. R. Gord, B. S. Freiser, *J. Am. Chem. Soc.* **1988**, *110*, 6606.

[74] a) M. Brönstrup, I. Kretzschmar, D. Schröder, H. Schwarz, *Helv. Chim. Acta* **1998**, *81*, 2348; b) R. Liyange, P. B. Armentrout, *Int. J. Mass Spectrom.* **2005**, *241*, 243.

[75] D. R. A. Ranatunga, Y. D. Hill, B. S. Freiser, *Organometallics* **1996**, *15*, 1242.

[76] a) G. C. Bond, D. J. Thompson, *Catal. Rev. Sci. Eng.* **1999**, *41*, 319, and references therein; b) for the role of gold catalysts in organic *synthesis*, see: G. Dyker, *Angew. Chem.* **2000**, *112*, 4407; *Angew. Chem. Int. Ed.* **2000**, *39*, 4237; c) A. S. K. Hashmi, *Gold Bull.* **2004**, *37*, 51.

[77] a) M. Haruta, N. Yamada, T. Kobayashi, S. Iijima, *J. Catal.* **1989**, *115*, 301; b) M. Haruta, *Catal. Today* **1997**, *36*, 153; c) M. Valden, X. Lai, D. W. Goodman, *Science* **1998**, *281*, 1647; d) A. Sanchez, S. Abbet, U. Heiz, W.-D. Schneider, H. Häkkinen, R. N. Barnett, U. Landman, *J. Phys. Chem. A* **1999**, *103*, 9573; e) U. Heiz, A. Sanchez, S. Abbet, W.-D. Schneider, *Eur. Phys. J. D* **1999**, *9*, 35; f) N. Lopez, J. K. Nørskov, *J. Am. Chem. Soc.* **2002**, *124*, 11262; g) M. S. Chen, D. W. Goodman, *Science*, **2004**, *306*, 252; h) for an essay on this topic, see: A. Cho, *Science* **2003**, *299*, 1684.

[78] For reviews, see: a) D. M. P. Mingos, T. Slee, L. Zhenyang, *Chem. Rev.* **1990**, *90*, 383; b) M. P. Irion, *Int. J. Mass Spectrom. Ion Processes* **1992**, *121*, 1; c) M. B. Knickelbein, *Annu. Rev. Phys. Chem.* **1999**, *50*, 79; d) J. A. Alonso, *Chem. Rev.* **2000**, *100*,

637; e) P. B. Armentrout, *Annu. Rev. Phys. Chem.* **2001**, *52*, 423; f) V. E. Bondybey, M. K. Beyer, *J. Phys. Chem. A* **2001**, *105*, 951; g) Y. D. Kim, *Int. J. Mass Spectrom.* **2004**, *238*, 17; h) T. M. Bernhardt, *Int. J. Mass Spectrom.*, in press.

[79] a) For an exhaustive collection of experimental/theoretical studies on metal clusters in general, see: *Metal Clusters in Chemistry* (Eds.: P. Braunstein, L. A. Oro, P. R. Raithby), Wiley, New York, **1999**; b) for a recent survey that contains 794 references on the chemistry of gold, see: P. Pyykkö, *Angew. Chem.* **2004**, *116*, 4512; *Angew. Chem. Int. Ed.* **2004**, *43*, 4412.

[80] For a selection of more recent studies, see: a) W. T. Wallace, R. L. Whetten, *J. Phys. Chem. B* **2000**, *104*, 10964; b) X. Wu, L. Senapati, S. K. Nayak, A. Selloni, M. Hajaligol, *J. Chem. Phys.* **2002**, *117*, 4010; c) J. Hagen, L. D. Socaciu, M. Elijazyfer, T. M. Bernhardt, L. Wöste, *Phys. Chem. Chem. Phys.* **2002**, *4*, 1707; d) I. Balteanu, O. P. Balaj, B. S. Fox, M. K. Beyer, Z. Bastl, V. E. Bondybey, *Phys. Chem. Chem. Phys.* **2003**, *5*, 1213; e) D. Stokic, M. Fischer, G. Ganteför, Y. D. Kim, Q. Sun, P. Jena, *J. Am. Chem. Soc.* **2003**, *125*, 2848; f) for the role of the charge of supported gold clusters in the low-temperature oxidation of CO, see: B. Yoon, H. Häkkinen, U. Landman, A. S. Wörz, J.-M. Antonietti, S. Abbot, K. Judai, U. Heiz, *Science* **2005**, *307*, 403.

[81] Y. D. Kim, M. Fischer, G. Ganteför, *Chem. Phys. Lett.* **2003**, *377*, 170.

[82] a) Y. Shi, K. M. Ervin, *J. Chem. Phys.* **1998**, *108*, 1575; b) a full catalytic cycle of CO oxidation with N_2O on cationic platinum clusters for Pt_n^+ ($n = 5$–10), including aspects of catalyst's poisoning by CO, has been reported recently: O. P. Bolaj, I. Balteanu, T. T. J. Roßteunscher, M. K. Beyer, V. E. Bondybey, *Angew. Chem.* **2004**, *116*, 6681; *Angew. Chem. Int. Ed.* **2004**, *43*, 6519; c) for the cluster-size-dependent reaction behavior of CO with O_2 on free, negatively charged silver anions, see: L. D. Socacin, J. Hagen, J. LeRoux, D. Popolan, T. M. Bernhardt, L. Wöste, and S. Vajda, *J. Chem. Phys.* **2004**, *120*, 2078, and references therein; d) in contrast to $Fe_2O_2^+$ which does not oxidize CO (O. Gehret, M. P. Irion, *Chem. Eur. J.* **1996**, *2*, 598; P. Jackson, J. N. Harvey, D. Schröder, H. Schwarz, *Int. J. Mass Spectrom.* **2001**, *204*, 233), $Ni_2O_2^+$ brings about efficient oxidation of CO. $Ni_2O_2^+$ can be conveniently generated by reaction of

Ni_2^+ with N_2O, and hence this is another example of cluster-mediated oxygen-atom transport catalysis in the N_2O/CO system. For details, see: K. Koszinowski, M. Schlangen, D. Schröder, H. Schwarz, *Eur. J. Inorg. Chem.*, in press.

[83] R. M. Heck, R. J. Farranto, *Catalytic Air Pollution Control: Commercial Technology*, Van Nortrand Reinhold, New York, **1995**.

[84] a) A. G. Sault, D. W. Goodman, *Adv. Chem. Phys.* **1989**, *76*, 153; b) S. L. Bernasek, *Heterogeneous Reaction Dynamics*, VCH, New York, **1995**.

[85] a) H. Häkkinen, U. Landman, *J. Am. Chem. Soc.* **2001**, *123*, 9704; b) W. T. Wallace, R. L. Whetten, *J. Am. Chem. Soc.* **2002**, *124*, 7499; c) L. D. Socaciu, J. Hagen, T. M. Bernhardt, L. Wöste, U. Heiz, H. Häkkinen, U. Landman, *J. Am. Chem. Soc.* **2003**, *125*, 10437; d) M. L. Kimble, A. W. Castleman, Jr., R. Mitrić, C. Bürgel, V. Bonačic-Koutecký, *J. Am. Chem. Soc.* **2004**, *126*, 2526; e) N. Lopez, J. K. Nørskov, *J. Am. Chem. Soc.* **2002**, *124*, 11262.

[86] G. Centi, F. Cavani, F. Trifiro, *Selective Oxidation by Heterogeneous Catalysis*, Kluwer Academic/Plenum Publishers, New York, **2001**.

[87] T. Waters, R. A. J. O'Hair, A. G. Wedd, *J. Am. Chem. Soc.* **2003**, *125*, 3384.

[88] W. E. Farneth, R. H. Staley, A. W. Sleight, *J. Am. Chem. Soc.* **1986**, *108*, 2327.

[89] B. Chiavarino, M. E. Crestoni, S. Fornarini, *Chem. Eur. J.* **2002**, *8*, 2740.

[90] a) T. Waters, R. A. J. O'Hair, A. G. Wedd, *Int. J. Mass Spectrom.* **2003**, *228*, 599; b) for an example of a catalytic cycle for the gas-phase decarboxylation of acetic acid by organomagnesates, see: R. A. J. O'Hair, A. K. Vrkic, P. F. James, *J. Am. Chem. Soc.* **2004**, *126*, 12173.

[91] M. A. Barteau, *Chem. Rev.* **1996**, *96*, 1413, and references therein.

[92] a) H. S. Taylor, *Proc. R. Soc. London A* **1925**, *108*, 105; b) G. M. Schwab, E. Pletsch, *Z. Phys. Chem.* **1929**, *131*, 385; c) R. J. Davis, *Science* **2003**, *301*, 926; d) Q. Fu, H. Saltsburg, M. Flytzani-Stephanopoulos, *Science* **2003**, *301*, 935; e) K. Horn, *Science* **2004**, *305*, 483.